heavy chain with the germlines revealed that the μ-chains of HO538-213 and HO702-001 were 95 and 97% homologous to germ line V_H3-33, respectively, while HO702-016 was 96% homologous to germline V_H4-4 [17]. For the light chains, the κ-chain Vkappa3 of HO538-213 was 97% homologous to germline L6 [6, 18, 19], and κ-chain Vkappa1 of both HO702-001 and HO702-016 was 97% homologous to the germline L12 [6, 18, 19]. These data suggest that there is a preferential use of V_H and V_L genes to develop CD4-reactive Ab, considering the number of V_H and V_L genes present before the Ig gene rearrangement. According to the sequence analysis, the V_H amino acid sequences of HO538-213 and HO702-001 carried distinct mutations, although both were derived from the same germline V_H3-33. The mutations were more frequent in the CDR regions (Fig. 2B and C, Supporting Information Fig. 3), which is characteristic of somatic hypermutation (SHM) associated with affinity maturation. Unlike most SHM, however, mutations involving G/C were not dominant.

A

Clone	Ig class	VH family	Closest germline	% identity	VL family	Closest germline	% identity
HO538-213	IgM	VH 3	VH3-33	95%	Vk3	L6	97%
HO702-001	IgM	VH 3	VH3-33	97%	Vk-1	L12	97%
HO702-016	IgM	VH 4	VH4-4	96%	Vk-1	L12	97%

B

Clone			Number of mutations associated with: A	G	C	T	Ins[1]	del[2]	GC involvement (%)[3]	Total	aa changes[4]	(%)
HO702-001	heavy chain	FR	3	2	1	0	0	0	66.6	6	2	33.3
		CDR	0	0	0	0	0	0	0.0	5	0	0.0
	light chain	FR	0	0	0	2	0	0	0.0	2	1	50.0
		CDR	1	0	0	0	6	0	0.0	7	0	0.0
		Total	4	2	1	2	11	0	33.3	20	3	15.0
HO702-016	heavy chain	FR	1	0	0	0	0	0	0.0	1	0	0.0
		CDR	0	2	1	0	11	0	100.0	4	0	0.0
	light chain	FR	0	0	0	2	0	0	0.0	2	1	50.0
		CDR	1	0	0	0	6	0	0.0	7	0	0.0
		Total	2	2	1	2	17	0	42.9	24	1	4.2
HO538-213	heavy chain	FR	2	1	1	4	0	0	25.0	8	3	37.5
		CDR	2	2	5	1	16	0	70.0	25	5	20.0
	light chain	FR	1	2	1	0	0	0	75.0	4	3	75.0
		CDR	3	1	0	0	2	0	25.0	6	3	50.0
		Total	8	6	7	6	17	0	60.0	43	13	30.2

C

Light chain

```
                    FR1                  CDR1          FR2           CDR2
HO538-213   EIVMTQSPATLSLSPGERATLSC  RASQSVNNYLA  WYQQKPGQAPSLLIY  DASNRAT
HO702-001/016 D-QL----S----A-V-D-V-IT-  ------ISSM--  ----K---K---K-----  K---SLES

                    FR3                  CDR3          FR4
HO538-213   GIPARFSGSGSGTDFTLTISSLEPEDFAVYYC  QQ.RG.NWPWT  FGQGTKLEIKRT
HO702-001/016 -V-S---------E----------Q-D----Y----  --YNSYSRTY-  ------------
```

Heavy chain

```
                    FR1                  CDR1          FR2           CDR2
HO538-213   QVQLVQSGGGVVQPGRSLRLSCA.ASG.FTFS  SYGMH  WVRQAPGKGLEWVA  VVCYDGRTTYYADSVKG
HO702-001   -----QEM-------------------------  -----  ----------------  --IN---SNK---------
HO702-016   -----QE---P-L-K-SQT-S-Y-TVSG-SISSG  --YWS  -I---PA-------IG  .RI-TSGS-N-MP-L-S

                    FR3                  CDR3          FR4
HO538-213   RFTISRDISENTLYLQMNSLRAEDTAVYYCAK  DLWKGYCNNGGCYG.VDC  WGQGTLVTVSS
HO702-001   ---------N-K-------------------R  -..RD..SG-S---SWF-P  ------------
HO702-016   -V---SW-T-K-QFS-KLS-VT-A--------R  T..PTL.GR-L.F....Y  ------------
```

Figure 2. Genetic analysis of CD4-reactive Ab. (A) Summary of the Ig class, V-gene family, closest germ line, and percentage identity of the closest germ line of CD4-reactive Ab. (B) The mutation profiles of the CD4-reactive IgM Fab fragments. (C) The deduced protein sequences of the V_H and V_L genes of the CD4-reactive Fab fragments are aligned. FR, framework region. Dashes and dots indicate identical residues and deletions, respectively. See Supporting Information Fig. 2 for further detail.

Inhibition of HIV replication by a Fab fragment of a CD4-reactive IgM

We next examined the potential impact of these CD4-reactive Fab Ab on HIV replication. Viral replication was monitored in PBMC by measuring $p24^{CA}$ viral Ag levels in the culture supernatant. Among the three IgM Fab clones, HO538-213 suppressed R5-tropic virus HIV-1_{JR-FL} replication by 3.5±1.5-fold at 1–2.5 μg/mL (average±SD from four independent experiments, Fig. 3A). There was a modest but consistent suppression of X4-tropic virus HIV-1_{HXB2} replication (1.4±0.2-fold, average±SD from three independent experiments). BIACORE and ELISA revealed that HO538-213 did not compete with the anti-CD4 mAb Leu-3a [20, 21] for CD4 binding. Leu-3a restricts HIV-1 replication by physically blocking the *Env*-CD4 interaction (data not shown), suggesting that the epitope recognized by HO538-213 is distinct from the *Env*-interacting domain of CD4 [7, 22, 23]. The monoclonal anti-CD4 Ab OKT4a does not block the *Env*-CD4 interaction, but restricts HIV-1 infection, although decreasing CD4 lateral diffusion on the cell surface [24–26]. We hypothesized that HO538-213 may have a similar mechanism of action. CD4 localizes to lipid rafts, and CD4-crosslinking activates signal transduction involving tyrosine kinases [27–29]. Thus, we treated MOLT-4 cells with HO538-213, and the lipid raft fraction was isolated by a membrane floatation assay as verified by the raft markers glycosphingomyelin 1 and sphingomyelin (Fig. 3B, left panel). Tyrosine kinase activitiy was examined by immunoblotting the lipid raft fractions using a PY20 anti-phosphotyrosine mAb (Fig. 3B, right panel, arrowhead). We detected a significant amount of tyrosine phosphorylation in the lipid raft fraction after HO538-213 treatment, indicating that HO538-213 can assemble cell surface CD4. This is consistent with our hypothesis that HO538-213 inhibits HIV-1 infection by decreasing the lateral movement of cell surface CD4.

Does CD4-reactive IgM function as a natural HIV resistance factor?

We then further characterized the donor from which the CD4-reactive Ab was isolated. The donor serum did not show a strong reactivity to rhCD4 at 1:10 dilution, where the non-specific effect was no longer detected. We analyzed the HIV-inhibition titer of the donor plasma. In a TZM-bl cell assay, the plasma did not block HIV replication at 1:50 dilution (data not shown). These data suggest that the CD4-reactive IgM circulates at very low titers in the donor and may not be sufficient to block HIV infection *in vitro*. However, it is possible that the CD4-reactive IgM may be able to limit HIV-1 propagation under *in vivo* conditions.

We next investigated the immunological status of the donor. IgG and IgM levels were within the normal range, and the plasma was negative for rheumatoid factor, anti-DNA, and anti-ribonucleoprotein Ab. However, the donor serum reacted to nuclear Ag at a titer of 1:160 (1:40 or less is considered normal), and the staining patterns were nucleolar (1:160) and speckled (1:80). Consistent with these data, the frequency of auto-reactive

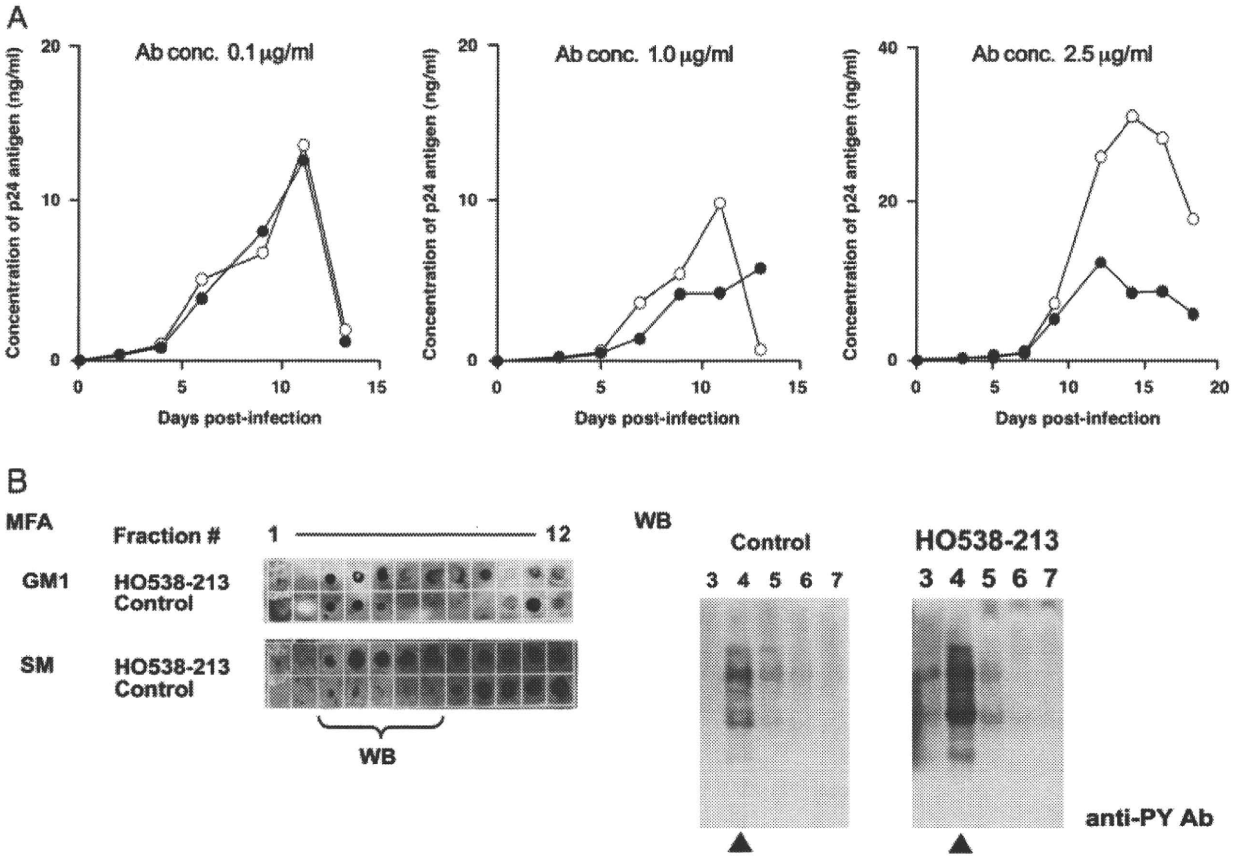

Figure 3. The effect of CD4-reactive Fab clone HO538-213 on HIV-1 replication. (A) The Fab clone HO538-213 (filled circles) was tested for its ability to inhibit HIV-1_{JR-FL} replication at a concentration of 0.1 (left), 1.0 (middle), and 2.5 (right) μg/mL. The CD4 non-reactive Fab clone 13-3 (open circles) was used as a negative control. Representative data from four independent experiments are shown. (B) Activation of the tyrosine kinase signaling cascade by HO538-213 in MOLT-4 cells. The detergent-resistant membrane fraction (arrowhead) was isolated by a membrane floatation assay (MFA) from MOLT-4 cells treated with HO538-213, and phosphotyrosine levels were examined by immunoblotting. GM1, glycosphingomyclin 1; SM, sphingomyelin.

Ab-producing cells from the same donor, namely against nuclear Ag and blood group i-glycolipid, was significantly higher than the other donors (Fig. 1A). In addition, we isolated anti-TNF-α IgG and IgM clones from this donor [16]. Although clinical manifestations of autoimmune disorders were lacking, it is likely that the donor may have an immunological background that generates auto-reactive Ab and tolerates them. Moreover, the donor has been healthy for 29 years, at the time the CD4-reactive Ab was first isolated, suggesting that such CD4-reactive Ab may not disturb host immunity.

Considering that the IgM-producing B cells we isolated went through positive/negative selection, their original target should not be CD4. It is thus likely that the IgM genes accumulated SHM that resulted in cross-reactivity to CD4 in the periphery after B-cell maturation. To better understand the unique immunological features of individuals with CD4-reactive Ab and their auto-reactive Ab repertoire, more human monoclonal self-reactive Ab are needed to analyze both their V-region sequences and cross-reactivities. Our experimental approach might be useful for addressing these issues. Unfortunately, however, we were unable to characterize the CD4-reactive Ab-producing cells, as the oligoclonal cultures of B-LCL were terminated after RNA extraction for our Ig gene cloning strategy. We speculate that B-1 cells could be the source of the CD4-reactive Ab, because B-1 cells produce IgM that often cross-reacts with auto-Ag.

Our genetic data indicated that only a fraction of the CD4-reactive Ab could have some HIV-inhibitory function. It is an open question whether such CD4-reactive HIV-inhibitory Ab may be present in the other healthy individuals, as well as in HIV-seropositive long-term non-progressors.

HIV-inhibitory CD4-reactive Ab are effective against multiple HIV clades, as CD4 is the major HIV receptor for all the viral clades [11]. A clinical trial is being conducted to examine the therapeutic efficacy of a humanized CD4-reactive mAb in patients with HIV infection [8, 12]. Although CD4-reactive Ab can be detected in healthy individuals, safety is always a concern when using self-recognizing Ab as therapeutic drugs. Given that HO538-213 was isolated from a healthy individual and that it recognized a different epitope than Leu-3a, HO538-213 might effectively inhibit HIV without disturbing $CD4^+$ T-cell functions. As noted above, the donor from which the three CD4-reactive IgM Fab were isolated has been healthy for more than 29 years since PBMC collection, suggesting that these Ab may not seriously inhibit $CD4^+$ T-cell functions *in vivo* and thus may be useful in treating HIV infection and other disorders [4].

Concluding remarks

This report provides the first clonal genetic analyses of human monoclonal anti-CD4 Ab. IgM is considered to function in "natural humoral immunity", as it has a relatively low affinity for pathogens and confers natural resistance to infectious agents. However, the pathogen-specific immunity function of IgM has not been demonstrated at a clonal level. Our data suggest that CD4-reactive IgM is present in healthy individuals and can contribute to natural resistance to HIV infection and AIDS progression. This is the first clear demonstration of a natural humoral immunity function of IgM against HIV.

Materials and methods

Functional cloning of heavy and light chain Ab genes

The establishment of Ab-producing cells, cloning of Ig genes encoding V regions, ELISA, and the purification of Fab fragments from *Escherichia coli* have been described previously [16]. The experimental procedure is schematically shown in the Supporting Information Fig. 1. In brief, PBMC from 12 donors, including two healthy individuals and ten individuals with autoimmune disorders, were infected with the B95-8 strain of EBV, and 1×10^4 cells were propagated in 96-well plates. The supernatant was analyzed by ELISA using rhCD4 derived from a baculovirus system (50 ng/well; INTRACELL) as an Ag. Other Ag tested, including viral, bacterial, and auto-Ag, are listed in the Supporting Information Fig. 2. Total cellular RNA was isolated from oligoclonal cell populations positive for anti-CD4 Ab production (RNeasy mini kit, Qiagen). cDNAs were synthesized and amplified by PCR with specific primers for human Ig μ-, γ-, λ-, and κ-chains. Only the μ- and κ-chains were amplified from HO538 and HO702 cultures and cloned into the pFab1-His2 vector, generating bacterial Fab-expression libraries [30]. The pFab libraries were screened for the production of CD4-reactive Fab by ELISA. The Fab fragments were purified using an anti-Fab Ab affinity column. The eluted Fab was dialyzed against PBS and concentrated by centrifugation (VIVASPIN concentrator, Vivascience AG). The purity of the Fab Ab was greater than 95% as determined by SDS-PAGE analysis (data not shown).

Surface plasmon resonance biosensor analysis

Surface plasmon resonance analyses were performed using BIACORE 3000 (GE Healthcare). The hrCD4 was immobilized onto CM5 sensor chips using standard amine-coupling chemistry. The purified Fab was diluted in a running buffer (10 mM HEPES, 0.15 M NaCL, 3 mM EDTA, surfactant P 20, pH 7.4) to 0.3–20 μg/mL and injected at a rate of 20–30 μL/min. The Fab was allowed to associate and dissociate for 120–270 s.

Cells

B-LCL and 293 T cells were maintained in Roswell Park Memorial Institute (RPMI) 1640 (Sigma) supplemented with 10% fetal bovine serum (Japan Bioserum), penicillin, and streptomycin (Invitrogen). The primary mononuclear cells were maintained in RPMI 1640 supplemented with 10% fetal bovine serum, penicillin, streptomycin, 5 μg/mL plasmocin (InvivoGen), 10 mM HEPES, 5 μg/mL anti-CD3 mAb (OKT3, Janssen Pharmaceutical), 70 U/mL recombinant human IL-2 (Shionogi Pharmaceutical), GlutaMax-I (Invitrogen), insulin–transferrin–selenium-A (Invitrogen), and 10 mM HEPES (Invitrogen). Cells were incubated at 37°C in a humidified 5% CO_2 atmosphere.

Other experimental procedures

Procedures for monitoring HIV-1 replication [31] and membrane floatation assays [32] were described previously. Standard auto-Ab was tested by the clinical laboratory testing service SRL (Tokyo, Japan).

Acknowledgements: The authors thank Hideo Tsukamoto for BIACORE analysis. This work was supported by the Japan Health Science Foundation, the Japanese Ministry of Health, Labor and Welfare (H18-AIDS-W-003 to JK), and the Japanese Ministry of Education, Culture, Sports, Science and Technology (18689014 and 18659136 to JK).

Conflict of interest: The authors declare no financial or commercial conflict of interest.

References

1 **Henriksson, G., Manthorpe, R. and Bredberg, A.,** Antibodies to CD4 in primary Sjogren's syndrome. *Rheumatology (Oxford)* 2000. **39**: 142–147.

2 **Lenert, P., Lenert, G. and Senecal, J. L.,** CD4-reactive antibodies in systemic lupus erythematosus. *Hum. Immunol.* 1996. **49**: 38–48.

3 **Lopalco, L., Magnani, Z., Confetti, C., Brianza, M., Saracco, A., Ferraris, G., Lillo, F. et al.,** Anti-CD4 antibodies in exposed seronegative adults and in newborns of HIV type 1-seropositive mothers: a follow-up study. *AIDS Res. Hum. Retroviruses* 1999. **15**: 1079–1085.

4 **Herzog, C., Walker, C., Muller, W., Rieber, P., Reiter, C., Riethmuller, G., Wassmer, P. et al.,** Anti-CD4 antibody treatment of patients with rheumatoid arthritis: I. Effect on clinical course and circulating T cells. *J. Autoimmun.* 1989. **2**: 627–642.

5 **Rieber, E. P., Federle, C., Reiter, C., Krauss, S., Gurtler, L., Eberle, J., Deinhardt, F. and Riethmuller, G.,** The monoclonal CD4 antibody M-T413 inhibits cellular infection with human immunodeficiency virus after viral attachment to the cell membrane: an approach to postexposure prophylaxis. *Proc. Natl. Acad. Sci. USA* 1992. **89**: 10792–10796.

6 **Bentley, D. L. and Rabbits, T. H.,** Human immunoglobulin variable region genes – DNA sequences of two V kappa genes and a pseudogene. *Nature* 1980. **288**: 730–733.

7 **Moir, S., Lapointe, R., Malaspina, A., Ostrowski, M., Cole, C. E., Chun, T. W., Adelsberger, J. et al.,** CD40-Mediated induction of CD4 and CXCR4 on B lymphocytes correlates with restricted susceptibility to human immunodeficiency virus type 1 infection: potential role of B lymphocytes as a viral reservoir. *J. Virol.* 1999. **73**: 7972–7980.

8 **Kuritzkes, D. R., Jacobson, J., Powderly, W. G., Godofsky, E., DeJesus, E., Haas, F., Reimann, K. A. et al.,** Antiretroviral activity of the anti-CD4 monoclonal antibody TNX-355 in patients infected with HIV type 1. *J. Infect. Dis.* 2004. **189**: 286–291.

9 **Burastero, S. E., Gaffi, D., Lopalco, L., Tambussi, G., Borgonovo, B., De Santis, C., Abecasis, C. et al.,** Autoantibodies to CD4 in HIV type 1-exposed seronegative individuals. *AIDS Res. Hum. Retroviruses* 1996. **12**: 273–280.

10 **Boon, L., Holland, B., Gordon, W., Liu, P., Shiau, F., Shanahan, W., Reimann, K. A. and Fung, M.,** Development of anti-CD4 MAb hu5A8 for treatment of HIV-1 infection: preclinical assessment in non-human primates. *Toxicology* 2002. **172**: 191–203.

11 **Shearer, M. H., Timanus, D. K., Benton, P. A., Lee, D. R. and Kennedy, R. C.,** Cross-clade inhibition of human immunodeficiency virus type 1 primary isolates by monoclonal anti-CD4. *J. Infect. Dis.* 1998. **177**: 1727–1729.

12 **Hurez, V., Kaveri, S. V., Mouhoub, A., Dietrich, G., Mani, J. C., Klatzmann, D. and Kazatchkine, M. D.,** Anti-CD4 activity of normal human immunoglobulin G for therapeutic use. (Intravenous immunoglobulin, IVIg). *Ther. Immunol.* 1994. **1**: 269–277.

13 **Bomsel, M., Pastori, C., Tudor, D., Alberti, C., Garcia, S., Ferrari, D., Lazzarin, A. and Lopalco, L.,** Natural mucosal antibodies reactive with first extracellular loop of CCR5 inhibit HIV-1 transport across human epithelial cells. *AIDS* 2007. **21**: 13–22.

14 **Sugden, B. and Mark, W.,** Clonal transformation of adult human leukocytes by Epstein–Barr virus. *J. Virol.* 1977. **23**: 503–508.

15 **Takekoshi, M., Maeda, F., Tachibana, H., Inoko, H., Kato, S., Takakura, I., Kenjyo, T. et al.,** Human monoclonal anti-HCMV neutralizing antibody from phage display libraries. *J. Virol. Methods* 1998. **74**: 89–98.

16 **Takekoshi, M., Maeda, F., Nagatsuka, Y., Aotsuka, S., Ono, Y. and Ihara, S.,** Cloning and expression of human anti-tumor necrosis factor-alpha monoclonal antibodies from Epstein–Barr virus transformed oligoclonal libraries. *J. Biochem.* 2001. **130**: 299–303.

17 **Matsuda, F., Ishii, K., Bourvagnet, P., Kuma, K., Hayashida, H., Miyata, T. and Honjo, T.,** The complete nucleotide sequence of the human immunoglobulin heavy chain variable region locus. *J. Exp. Med.* 1998. **188**: 2151–2162.

18 **Huber, C., Schable, K. F., Huber, E., Klein, R., Meindl, A., Thiebe, R., Lamm, R. and Zachau, H. G.,** The V kappa genes of the L regions and the repertoire of V kappa gene sequences in the human germ line. *Eur. J. Immunol.* 1993. **23**: 2868–2875.

19 **Pech, M. and Zachau, H. G.,** Immunoglobulin genes of different subgroups are interdigitated within the VK locus. *Nucleic Acids Res.* 1984. **12**: 9229–9236.

20 **Healey, D., Dianda, L., Moore, J. P., McDougal, J. S., Moore, M. J., Estess, P., Buck, D. et al.,** Novel anti-CD4 monoclonal antibodies separate human immunodeficiency virus infection and fusion of CD4+ cells from virus binding. *J. Exp. Med.* 1990. **172**: 1233–1242.

21 **Peterson, A. and Seed, B.,** Genetic analysis of monoclonal antibody and HIV binding sites on the human lymphocyte antigen CD4. *Cell* 1988. **54**: 65–72.

22 **Benkirane, M., Hirn, M., Carriere, D. and Devaux, C.,** Functional epitope analysis of the human CD4 molecule: antibodies that inhibit human immunodeficiency virus type 1 gene expression bind to the immunoglobulin CDR3-like region of CD4. *J. Virol.* 1995. **69**: 6898–6903.

23 **Sattentau, Q. J., Dalgleish, A. G., Weiss, R. A. and Beverley, P. C.,** Epitopes of the CD4 antigen and HIV infection. *Science* 1986. **234**: 1120–1123.

24 **Pal, R., Nair, B. C., Hoke, G. M., Sarngadharan, M. G. and Edidin, M.,** Lateral diffusion of CD4 on the surface of a human neoplastic T-cell line probed with a fluorescent derivative of the envelope glycoprotein (gp120) of human immunodeficiency virus type 1 (HIV-1). *J. Cell. Physiol.*1991. **147**: 326–332.

25 **Finnegan, C. M., Rawat, S. S., Cho, E. H., Guiffre, D. L., Lockett, S., MerrillJr., A. H. and Blumenthal, R.,** Sphingomyelinase restricts the lateral diffusion of CD4 and inhibits human immunodeficiency virus fusion. *J. Virol.* 2007. **81**: 5294–5304.

26 **Rawat, S. S., Zimmerman, C., Johnson, B. T., Cho, E., Lockett, S. J., Blumenthal, R. and Puri, A.,** Restricted lateral mobility of plasma membrane CD4 impairs HIV-1 envelope glycoprotein mediated fusion. *Mol. Membr. Biol.* 2008. **25**: 83–94.

27 **Xavier, R., Brennan, T., Li, Q., McCormack, C. and Seed, B.,** Membrane compartmentation is required for efficient T cell activation. *Immunity* 1998. **8**: 723–732.

28 **Millan, J., Cerny, J., Horejsi, V. and Alonso, M. A.,** CD4 segregates into specific detergent-resistant T-cell membrane microdomains. *Tissue Antigens* 1999. **53**: 33–40.

29 **Nguyen, D. H., Giri, B., Collins, G. and Taub, D. D.,** Dynamic reorganization of chemokine receptors, cholesterol, lipid rafts, and adhesion molecules to sites of CD4 engagement. *Exp. Cell. Res.* 2005. **304**: 559–569.

30 **Maeda, F., Nagatsuka, Y., Ihara, S., Aotsuka, S., Ono, Y., Inoko, H. and Takekoshi, M.,** Bacterial expression of a human recombinant monoclonal antibody fab fragment against hepatitis B surface antigen. *J. Med. Virol.* 1999. **58**: 338–345.

31 **Shimizu, S., Urano, E., Futahashi, Y., Miyauchi, K., Isogai, M., Matsuda, Z., Nohtomi, K. et al.,** Inhibiting lentiviral replication by HEXIM1, a cellular negative regulator of the CDK9/cyclin T complex. *AIDS* 2007. **21**: 575–582.

32 **Nagatsuka, Y., Hara-Yokoyama, M., Kasama, T., Takekoshi, M., Maeda, F., Ihara, S., Fujiwara, S. et al.,** Carbohydrate-dependent signaling from the phosphatidylglucoside-based microdomain induces granulocytic differentiation of HL60 cells. *Proc. Natl. Acad. Sci. USA* 2003. **100**: 7454–7459.

Abbreviations: **B-LCL:** B-lymphoblastoid cell lines · **rhCD4:** recombinant human CD4 · **SHM:** somatic hypermutation

Full correspondence: Dr. Jun Komano, AIDS Research Center, National Institute of Infectious Diseases, 1-23-1 Shinjuku, Tokyo 162-864, Japan
Fax: +81-3-5285-1111
e-mail: ajkomano@nih.go.jp

Additional correspondence: Dr. Masataka Takekoshi, Department of Molecular Life Science, Division of Basic Molecular Science and Molecular Medicine, Tokai University School of Medicine, Isehara, Japan
e-mail: mtakekos@is.icc.u-tokai.ac.jp

Received: 2/4/2009
Revised: 22/12/2009
Accepted: 1/2/2010
Accepted article online: 16/2/2010

Dominant-negative derivative of EBNA1 represses EBNA1-mediated transforming gene expression during the acute phase of Epstein–Barr virus infection independent of rapid loss of viral genome

Yumi Kariya,[1,2] Makiko Hamatake,[1] Emiko Urano,[1] Hironori Yoshiyama,[3] Norio Shimizu[2] and Jun Komano[1,4]

[1]AIDS Research Center, National Institute of Infectious Diseases, Tokyo; [2]Department of Virology, Division of Medical Science, Medical Research Institute, Tokyo Medical and Dental University, Tokyo; [3]Research Center for Infection-associated Cancer, Institute for Genetic Medicine, Hokkaido University, Sapporo, Japan

(Received November 1, 2009/Revised November 30, 2009/Accepted December 6, 2009)

The oncogenic human herpes virus, the Epstein–Barr virus (EBV), expresses EBNA1 in almost all forms of viral latency. EBNA1 plays a major role in the maintenance of the viral genome and in the transactivation of viral transforming genes, including EBNA2 and latent membrane protein (LMP-1). However, it is unknown whether inhibition of EBNA1 from the onset of EBV infection disrupts the establishment of EBV's latency and transactivation of the viral oncogenes. To address this, we measured EBV infection kinetics in the B cell lines BALL-1 and BJAB, which stably express a dominant-negative EBNA1 (dnE1) fused to green fluorescent protein (GFP). The EBV genome was surprisingly unstable 1 week post-infection: the average loss rate of EBV DNA from GFP- and GFP-dnE1-expressing cells was 53.4% and 41.0% per cell generation, respectively, which was substantially higher than that of an 'established' *oriP* replicon (2–4%). GFP-dnE1 did not accelerate loss of the EBV genome, suggesting that EBNA1-dependent licensing of the EBV genome occurs infrequently during the acute phase of EBV infection. In the subacute phase, establishment of EBV latency was completely blocked in GFP-dnE1-expressing cells. In contrast, C/W promoter-driven transcription was strongly restricted in GFP-dnE1-expressing cells at 2 days post-infection. These data suggest that inhibition of EBNA1 from the onset of EBV infection is effective in blocking the positive feedback loop in the transactivation of viral transforming genes, and in eradicating the EBV genome during the subacute phase. Our results suggest that gene transduction of GFP-dnE1 could be a promising therapeutic and prophylactic approach toward EBV-associated malignancies. (*Cancer Sci* 2010)

The Epstein–Barr virus (EBV) is a risk factor in several malignant diseases including Burkitt's lymphoma and nasopharyngeal carcinoma.[1–4] The opportunistic B-cell lymphoma is becoming the major cause of death in AIDS patients in an era of highly active antiretroviral therapy (HAART), and EBV is associated with a significant portion of AIDS lymphoma cases.[5,6] Neither an EBV vaccine, nor specific antiviral agents against EBV are available; thus attention should be paid to the development of therapeutic agents against EBV.

EBV-encoded genes including EBNA1, EBNA2, and latent membrane protein (LMP-1) are potential molecular targets for the treatment of EBV-associated lymphomas because they play central roles in the process of malignant transformation.[7] We are interested in EBNA1 since it contributes to EBV oncogenesis in two ways: it supports the maintenance of the EBV genome in *cis* and enhances expression of viral oncogenes, including EBNA2 and LMP-1, in *trans*.[7–9] EBNA1 exerts its biological functions by binding to its cognate binding sites within the family of repeats (FR) and the dyad symmetry element (DS) located within the origin of replication (oriP) of EBV DNA. EBNA1 interacts with FR to enhance transcription from the viral C/W promoters (C/Wp) and to partition EBV DNA to daughter cells; and with DS to initiate DNA replication.[7–9]

Maintenance of the oriP replicon is stable once EBV latency has been established. The loss rate of established oriP plasmids is estimated at 2–4% per cell generation.[10,11] Interestingly, the loss rate of the oriP replicon is significantly higher in cells transiently transduced with oriP plasmids (>25% per cell generation) than in established cells.[12] In primary B cells, EBV DNA is lost rapidly within 2 days post-infection (~98.9%).[13] However, the loss rate of the EBV genome during a week post-infection in B cells remains to be quantified.

Upon EBV infection, the first viral genes expressed are the transactivators EBNA2 and EBNA-LP transcribed from Wp several hours after infection.[7] EBNA2 binds to the EBNA2-responsive elements and, in cooperation with EBNA-LP, enhances transcription from Cp, which leads to expression of all EBNA proteins, including EBNA1. EBNA1 binding to oriP activates C/Wp to boost viral latent gene expression, including the EBNAs and LMP-1. The viral gene transactivation positive feedback loop is established within a few days post-infection, and EBNA1 is one of the key factors that sustain this feedback loop during the acute phase of EBV infection.[14] In parallel, EBNA1 contributes to the establishment of the EBV genome as a licensed replicon. It may be possible to stop EBV infection by breaking the chain of EBNA1-dependent events and thus the EBV-mediated malignant transformation of infected cells. Previous studies have assessed the therapeutic potential of a dominant-negative derivative of EBNA1 (dnE1) in cells in which EBV latency was already established.[15,16] In this study, we critically assessed whether inhibition of EBNA1 limits the early stage of EBV infection in B cells. We provide evidence that expression of dnE1 strongly blocks the expression of virus-encoded oncogenes in acutely infected cells without accelerating EBV genome loss, and disrupts EBV latency in the subacute phase of EBV infection.

Materials and Methods

Cells. The 293T, EBV-negative Burkitt lymphoma cell line BJAB, EBV-positive Burkitt lymphoma cell line Daudi, EBV-transformed healthy donor-derived B lymphoblastoid cell line (B-LCL), and B acute lymphoblastic leukemia cell line BALL-1

[4]To whom correspondence should be addressed.
E-mail: ajkomano@nih.go.jp

doi: 10.1111/j.1349-7006.2009.01474.x

cells (kindly provided by Dr. Yokota, National Institute of Infectious Diseases, Tokyo, Japan) were maintained in RPMI-1640 medium (Sigma, St. Louis, MA, USA) supplemented with 10% fetal bovine serum (Japan Bioserum, Tokyo, Japan), 50 U/mL penicillin, 50 μg/mL streptomycin (Invitrogen, Tokyo, Japan), and incubated at 37°C in a humidified 5% CO_2 atmosphere.

Plasmids. The following primers were used to amplify dnE1 from p1160[17] by PCR: 5′-ACCGGTCTCGAGCAATTGCCA-CCATGCGGGGTCAGGGTGATGGAGG-3′ and 5′-GGATC-CTCGAGCGGCCGCTCACTCCTGCCCTTCCTCACC-3′. The GFP-dnE1 expression vector (pGD) was constructed by cloning the MfeI-XhoI fragment of the PCR product into the BglII-SalI sites of pEGFP-C1 (Clontech, Palo Alto, CA, USA). The MfeI and BglII sites were blunted with T7 RNA polymerase. The AgeI-BamHI fragment from pGD was cloned into the corresponding restriction sites of pCMMP eGFP[15,18] to generate pCMMP GFP-dnE1. The EBNA1 expression vector p1553, the FR-tk-luciferase reporter p985, and pLuciferase (pCMV-luc) have been described previously.[17–20]

Luciferase assay. The 293T cells, grown in 48-well plates, were co-transfected with the indicated plasmids using Lipofectamine 2000 according to the manufacturer's protocol (Invitrogen, Tokyo, Japan). Cells were replated in 96-well plates in triplicate at 2 h post-transfection. Luciferase activity was measured 48 h after transfection using the Steady-Glo Kit (Promega, Madison, WI, USA).

Murine leukemia virus (MLV) vector infection and cell sorting. MLV vectors were produced as described previously.[18] B cells (1×10^7 cells) were incubated with 2 mL of MLV preparation overnight at 4°C with continuous agitation. GFP-positive cells were collected using a FACS sorter (FACS Vantage; Becton Dickinson, San Jose, CA, USA) at 11 days post-infection.

Western blotting. Western blotting was performed as described previously.[21,22] The following reagents were used: anti-GFP (MsX Green Fluorescent Protein; Chemicon, Temecula, CA, USA) and Envision$^+$ Dual Link System-HRP (Dako, Glostrup, Denmark).

EBV infection and nucleic acid extraction. The EBV B95-8 strain was a generous gift from Dr Fujiwara's group at the National Research Institute for Child and Development (Tokyo, Japan). B cells (1×10^7 cells) were incubated with 100 μL of B95-8 EBV for 1 h at 37°C, and genomic DNA was extracted from half of the infected cells soon after infection (QIAamp DNA Mini Kit; Qiagen, Tokyo, Japan). At 15 h post-infection, half of the cells were washed once with PBS and incubated for 5 min in lysis buffer (10 mM Tris-HCl [pH7.4], 10 mM NaCl, 3 mM $MgCl_2$, and 0.5% NP-40). The nuclear fraction was collected by centrifugation for 5 min at 20.6 K × *g* (Kubota 3740; Kubota, Tokyo, Japan), and high molecular weight DNA was extracted (nuclear DNA). At 2 days post-infection and at later time points, high molecular weight DNA, or total RNA (PureLink Total RNA Blood Purification Kit; Invitrogen) was extracted from 1×10^6 or 3×10^6 cells, respectively, according to the manufacturer's protocol. After EBV infection, 10 μM aciclovir (Kayaku, Tokyo, Japan) was added to the culture medium. The production and infection of the recombinant EBV Akata strain carrying GFP and neomycin resistant genes has been described previously.[23] At 2 days post-infection, cells were plated at a density of 1×10^4 cells per well in a flat-bottomed 96-well plate, and cultured in a medium containing 1 mg/mL G418. The efficiency of EBV latency establishment was evaluated as percentage of wells positive for the emergence of G418-resistant cells at 2 to 3 weeks post-G418 selection.

Quantitative real-time PCR. Real-time PCR was performed as described previously; serial dilutions of positive controls were used as standards.[21] Amplifications were performed using the QuantiTect SYBR Green RT-PCR/PCR Kit (Qiagen), and the following primers: BamHI W repeat, 5′-GCCAGAGG-TAAGTGGACTTT-3′ and 5′-AGAAGCATGTATACTAAGC-CTCCC-3′; cyclophilin A (CYPA), 5′-CACCGCCACCATG-GTCAACCCCA-3′ and 5′-CCCGGGCCTCGAGCTTTCGAG-TTGTCCACAGTCAGCAATGG-3′; C/Wp, 5′-CCCTCGGA-CAGCTCCTAAG-3′ and 5′-CTTCACTTCGGTCTCCCCTA-3′; EBER1, 5′-AAAACATGCGGACCACCAGC-3′ and 5′-AG-GACCTACGCTGCCCTAGA-3′. The β-globin primers were described previously.[21] Following PCR amplification, the amplicons were separated in a 2% agarose gel, stained with ethidium bromide, and imaged with a Typhoon scanner (GE Healthcare Bio-Sciences; Piscataway, NJ, USA).

Results

Construction and functional verification of dnE1 fused to GFP. The carboxy half of EBNA1 serves as a functional dominant-negative inhibitor of EBNA1 that restricts the replication and maintenance of oriP plasmids as well as the EBNA1-dependent enhancement of transcription.[17,24] We used a dnE1 mutant encompassing amino acids 377 to 391 (the nuclear localization signal, NLS) and 451 to 641 (the DNA binding and dimerization domain) of EBNA1 (Fig. 1A).[17] To visualize the intracellular distribution of dnE1, we constructed the retroviral expression vector encoding GFP-dnE1. The expression of GFP-dnE1 was verified in transiently transfected 293T cells and stably transduced B cell lines using an MLV vector. To verify the function of GFP-dnE1, we conducted a reporter assay using a plasmid encoding the FR-tk-luciferase cassette. EBNA1 enhances expression of FR-tk-luciferase by binding to FR. If the GFP-dnE1 construct retains dnE1 function, co-expressing EBNA1 and GFP-dnE1 should reduce reporter activity. Luciferase activity was increased significantly upon EBNA1 expression by approximately 5.3-fold, consistent with previous findings (Fig. 1B, $P < 0.05$, two-tailed Student's *t*-test).[17] When GFP-dnE1 was co-expressed, the luciferase activity was decreased. The decrease in luciferase activity was proportional to the increase in GFP-dnE1 expression vector (Fig. 1B, maximum reduction: 22.3%, $P < 0.05$, two-tailed Student's *t*-test). This effect was not observed with GFP alone. In addition, CMV promoter-driven luciferase expression was unaffected by EBNA1, GFP-dnE1, and GFP, suggesting that the reduction in luciferase activity with GFP-dnE1 in the EBNA1/FR-tk-luciferase system is specific. These data indicate that GFP-dnE1 functions as an inhibitor of EBNA1.

Establishment of B cells constitutively expressing GFP-dnE1. To investigate the potential effect of GFP-dnE1 on EBV infection in B cells, we established BALL-1 and BJAB cells, which constitutively express GFP-dnE1, using an MLV vector. GFP was used as a control throughout this study. The distribution of GFP-dnE1 was examined by confocal microscopy, which revealed an even distribution of GFP throughout the cell. In contrast, the majority of GFP-dnE1was localized to the nucleus due to the presence of the NLS (Fig. 2A). Similar observations were made in BJAB and 293T cells (data not shown). We sorted the GFP- or GFP-dnE-expressing cells using a FACS sorter. To test the dose-dependent effect, we collected BALL-1 cell populations bearing high or low levels of GFP fluorescence, denoted as Hi and Lo, respectively. The expression of GFP and GFP-dnE1 was verified by Western blotting, which confirmed that GFP and GFP-dnE1 Hi cells had higher intensity signals than the GFP and GFP-dnE1 Lo cells (Fig. 2B). The rate of cell proliferation and the morphology of GFP-dnE1 cells were indistinguishable from those of GFP cells (Fig. 2A and data not shown).

Effect of GFP-dnE1 on the nuclear translocation of EBV DNA during the acute phase of EBV infection. To assess whether GFP-dnE1 could restrict the nuclear targeting of the EBV

doi: 10.1111/j.1349-7006.2009.01474.x

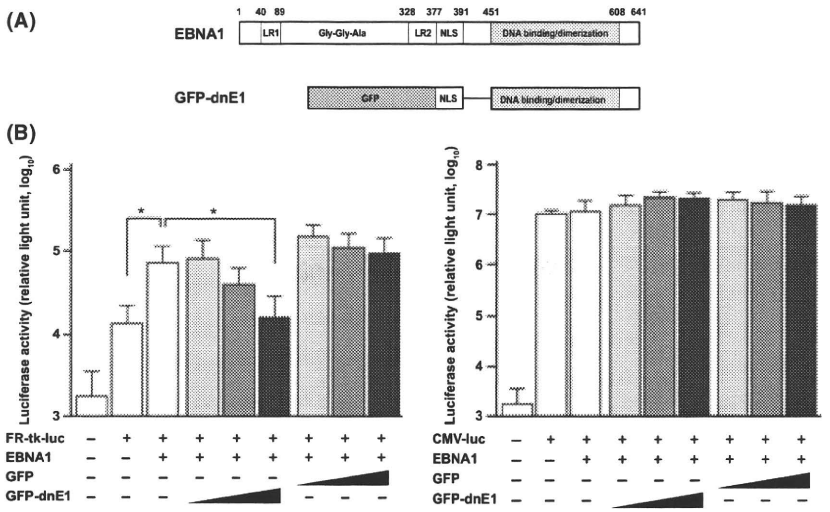

Fig. 1. Construction and functional characterization of a dominant-negative EBNA1 mutant (dnE1) fused to green fluorescent protein (GFP). (A) Structure of the EBNA1 protein and dnE1 used in this study. The linking regions (LR1 and LR2), the Gly-Gly-Ala repeat, the nuclear localization signal (NLS), and the DNA binding and dimerization domain are shown. GFP-dnE1 encodes the NLS and DNA binding and dimerization domain of EBNA1 fused to the C-terminus of GFP. (B) Repression of EBNA1-dependent transcriptional activation by GFP-dnE1. We transfected 293T cells in 48-well plates with 200 ng of FR-tk-luc or CMV-luc reporter, and 500 ng of EBNA1 expression vector, along with increasing amounts of GFP or GFP-dnE1 expression vector (20, 100, and 500 ng, respectively). $*P < 0.05$, two-tailed Student's *t*-test.

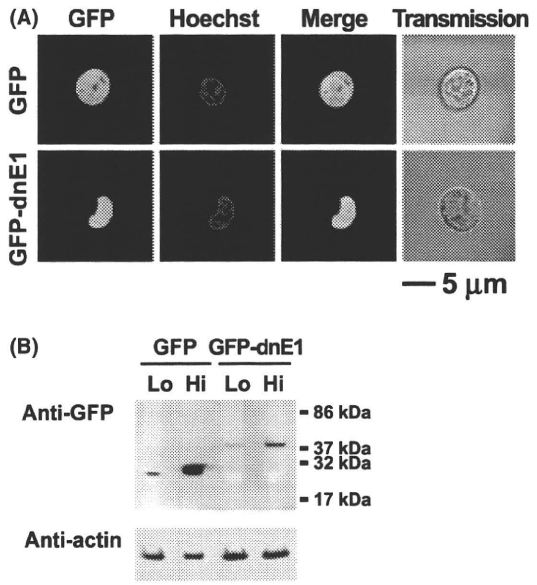

Fig. 2. Verification of stable green fluorescent protein (GFP)-dominant-negative EBNA1 (dnE1) expression in BALL-1 cells. (A) Distribution of GFP and GFP-dnE1 in BALL-1 cells was examined by confocal microscopy. Cells were imaged unfixed using a confocal microscope META 510 (Carl Zeiss, Tokyo, Japan). The green signal represents GFP fluorescence, and blue represents the Hoechst-stained nucleus. The bar represents 5 μm; magnification, ×630. (B) GFP or GFP-dnE1 expression in stably transduced BALL-1 cells was examined by Western blot analysis using an anti-GFP antibody. Protein lysates from 5×10^5 cells were loaded for each sample, except GFP Hi cells (5×10^4). The molecular weight marker is shown on the right.

genome after infection, we measured the amount of EBV DNA recovered from cells immediately after infection (representing the amount of EBV attached to cells) and the amount of EBV DNA that had migrated into the nucleus at 1 day post-infection. We isolated the nuclear fraction to exclude EBV DNA that failed to enter the nucleus. The number of EBV DNA molecules per cell was estimated by real-time PCR, which targeted the BamHI W repeat, in 10 ng of genomic DNA. We estimated the number of EBV DNA per cell given that a single cell contains approximately 10 pg of genomic DNA, and an EBV DNA has 10 copies of BamHI W repeats on average. The nuclear targeting efficiencies of EBV DNA were as follows: BALL-1 GFP cells, 43.3–108.6%; GFP-dnE1 cells, 46.9–65.6%; BJAB GFP cells, 37.4%; GFP-dnE1 cells, 35.0% (Table 1). These data suggested that the effect of GFP-dnE1 on the nuclear targeting of EBV DNA should be assessed more sensitively in BALL-1 and BJAB cell systems than in primary B cells because the nuclear targeting efficiency of EBV DNA in primary B cells is extremely inefficient (~1.1%).[13] In our experimental systems, the nuclear targeting efficiencies of EBV DNA in GFP-dnE1-expressing cells were similar to those in GFP-expressing cells. In addition, the dose-dependency of GFP-dnE1 was not observed in BALL-1 cells (Table 1). These data suggest that the nuclear targeting efficiency of EBV DNA was not restricted by the presence of GFP-dnE1 in B cells upon EBV infection.

Effect of GFP-dnE1 on the rate of loss of EBV DNA during the acute phase of EBV infection. To examine the effect of GFP-dnE1 on the rate of loss (ROL) of EBV DNA during the acute phase of viral infection, we monitored the EBV DNA copy number from day 2 to day 5 or day 6 post-infection, by real-time PCR, which detects the viral genome in both linear and circular configurations (Table 1). The ROL was estimated as the percentage reduction of EBV DNA per cell generation, considering that the cell doubling time is 24 h, and the kinetics of viral genome loss follows an exponential decay. The ROL in GFP-dnE1-expressing cells (19.2–85.9% per cell generation) was similar to GFP-expressing cells (20.5–79.4% per cell generation) in both BALL-1 and BJAB cells. In addition, there was no detectable dose-dependent effect of GFP-dnE1 in BALL-1 cells (Table 1 and Fig. 3). The averages ± SEs of ROL in GFP- and GFP-dnE1-expressing cells from six independent measurements in BALL-1 cells were 37.7 ± 10.7% and 25.7 ± 6.5% per cell generation, respectively (data not shown), which was substantially higher than the rate of loss of an established oriP replicon (2–4%).[10,11] These results reflect the precipitous loss of oriP plas-

Table 1. The kinetics of EBV DNA in the acute phase of EBV infection

Cell	Copy number of EBV DNA per cell at the indicated day†				Nuclear transport (%‡)	Rate of loss of EBV DNA (% per cell generation§)
Expt 1						
BALL-1	Day 0	Day 1	Day 2	Day 5		
GFP Hi	20.38	11.92	3.57	0.01¶	58.5	85.9
GFP Lo	17.26	11.68	3.21	0.56	67.7	44.1
GFP-dnE1 Hi	23.02	10.79	3.30	0.30	46.9	54.9
GFP-dnE1 Lo	18.83	12.36	1.46	0.53	65.6	28.7
BJAB	Day 0	Day 1	Day 2	Day 5		
GFP	155.1	58.8	5.38	0.06	37.4	77.7
GFP-dnE1	64.6	37.4	5.69	0.05	58.0	79.4
Expt 2						
BALL-1	Day 0	Day 1	Day 2	Day 6		
GFP Hi	16.33	17.73	11.10	4.74	108.6	19.2
GFP Lo	17.35	7.51	8.75	1.13	43.3	40.1
GFP-dnE1 Hi	18.46	8.71	8.95	3.38	47.2	21.6
GFP-dnE1 Lo	14.14	7.05	6.97	2.79	49.9	20.5

†Nuclear DNA was used for day 1 data. ‡Estimated from day 0 and day 1 data. §Estimated from day 2 and day 5 or day 6 data with the exponential decay. ¶Below the limit of detection. dnE1, dominant-negative EBNA1; EBV, Epstein–Barr virus; GFP, green fluorescent protein.

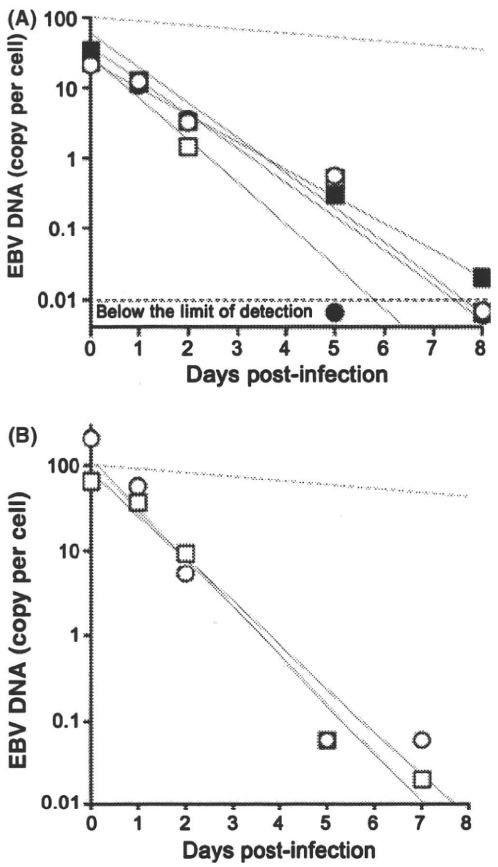

Fig. 3. Kinetics of Epstein–Barr virus (EBV) DNA loss during the acute phase of EBV infection. (A) Representative data from BALL-1 cells (Expt. 1 in Table 1) is shown. The filled squares, open squares, filled circles, and open circles represent GFP Hi, GFP Lo, GFP-dnE1 Hi, and GFP-dnE1 Lo, respectively. The limit of detection was below 0.01 (dashed line). The gray lines represent an approximation to the exponential decay. The dashed gray line represents the 4% rate of loss per cell generation. (B) Representative data from BJAB cells shown in Table 1. The circles and squares represent GFP and GFP-dnE1, respectively. Please see Table 1 for the detailed analysis.

mids (26–37%) in transiently transfected non-B cells.[12] The data suggest that GFP-dnE1 is unable to accelerate the ROL in the acute phase of EBV infection in B cells, presumably because the EBV genome is not established as an EBNA1-dependent stable licensed replicon. It should be noted that this is the first time that quantitative ROL data has been obtained by introducing the oriP replicon into B cells via EBV infection, which is an approach that does not confer any selective advantage on the infected cells.

Effect of GFP-dnE1 on efficiency of establishment of EBV latency. Cells infected with recombinant EBV, carrying the neomycin resistance gene, were seeded at 5×10^3 cells per well into a 96-well plate, and the efficiency of the establishment of EBV latency was assessed as the percentage of wells positive for the emergence of G418-resistant cells. G418-resistant cells appeared in BJAB, Daudi, parental BALL-1, and BALL-1 GFP cells at 56–100% efficiencies. In sharp contrast, G418-resistant cells were absent from GFP-dnE1-expressing BALL-1 cells (Table 2). These data clearly suggest that, although the ROL during the acute phase of EBV infection was not enhanced by GFP-dnE1, GFP-dnE1 was able to block the establishment of EBV latency completely during the subacute phase of EBV infection.

Effect of GFP-dnE1 on EBV-encoded latent gene expression. EBV gene expression was tested at 2 days post-infection by quantitative RT-PCR. We focused on the C/Wp activity because it expresses key viral transactivators including EBNA1, -2, -3s, and -LP to boost viral transforming gene expression. We detected C/Wp-driven transcripts in GFP Hi BALL-1 cells as expected. Conversely, C/Wp-driven transcripts were undetectable in GFP-dnE1 Hi and Lo BALL-1 cells, although these cells retained similar EBV DNA levels to GFP-expressing cells (Fig. 4 and Table 3). The Cp-driven transcript was under the limit of detection by RT-PCR, suggesting that the Wp is predominantly activated at the early phase of EBV infection consistent with previous findings.[7] Inhibition of viral gene transcription was not observed in the RNA polymerase III-driven transcript EBER1,[25] and cyclophilin A mRNA levels were similar between GFP- and GFP-dnE1-expressing cells (Fig. 4 and Table 3). This indicates that the effect of GFP-dnE1 on C/Wp activity is specific, and uncovers an active role of EBNA1 in supporting transactiva-

doi: 10.1111/j.1349-7006.2009.01474.x

Table 2. The establishment efficiency of EBV latency

Cell	Emergence of G418-resistant cells†	
BJAB	100%	(6/6)
Daudi	100%	(10/10)
BALL-1		
Parental	56%	(5/9)
GFP Hi	67%	(2/3)
GFP-dnE1 Hi	0%	(0/6)
GFP-dnE1 Lo	0%	(0/6)

†Percentage of wells positive for G418-resistant cells over the number of tested wells from 96-well plates indicated in the bracket. Shown are the sum of two independent experiments. dnE1, dominant-negative EBNA1; EBV, Epstein–Barr virus; GFP, green fluorescent protein.

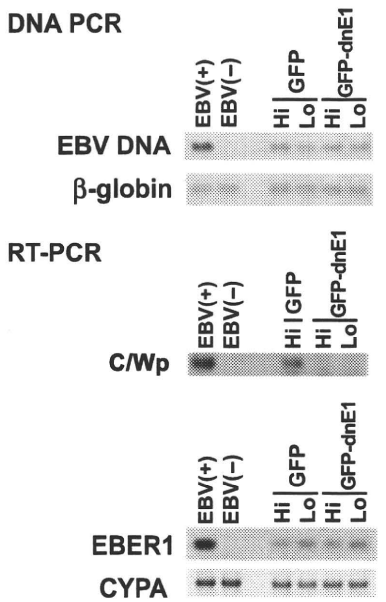

Fig. 4. PCR-based analysis of Epstein–Barr virus (EBV) gene expression. The effect of green fluorescent protein (GFP)-dominant-negative EBNA1 (dnE1) on the loss of EBV DNA (DNA PCR, upper panels) and transcription of the C/W promoter-driven transcript (C/Wp), EBER1, and cyclophilin A (CYPA; RT-PCR, lower panels) in BALL-1 cells at 2 days post-infection were examined. EBV-transformed B-lymphoblastoid cell line (B-LCL) and BJAB cells, denoted as EBV(+) and EBV(−), were used as positive and negative controls for viral DNA and RNA shown, respectively. β-Globin and CYPA were used as controls.

Table 3. Quantification of EBV transcripts in BALL-1 cells by real-time PCR at 2 days post-infection

BALL-1 cells		W1/2 exon (copies†)	EBER1 (copies‡)	CYPA (copies‡)
GFP	Hi	2.2	2.8×10^2	1.4×10^6
	Lo	NT§	0.8×10^2	1.0×10^6
GFP-dnE1	Hi	BLD¶	3.3×10^2	1.3×10^6
	Lo	BLD¶	1.2×10^2	1.5×10^6

†Copies per 13–14 ng total cellular RNA. ‡Copies per 200 ng total cellular RNA. §Not tested. ¶Below the limit of detection. CYPA, cyclophilin A; dnE1, dominant-negative EBNA1; EBV, Epstein–Barr virus; GFP, green fluorescent protein.

tion from C/Wp. Taken together, these results show that inhibition of EBNA1 functions strongly restricts EBV-encoded transforming gene expression and, although there is no detectable effect on the ROL of EBV DNA at the acute phase of viral infection, it blocks the establishment of EBV latency during the subacute phase.

Discussion

This is the first report describing the effect of EBNA1 inhibition from the onset of EBV infection in B cells. Unexpectedly, the dnE1 was unable to accelerate the ROL during the acute phase of EBV infection since dnE1 enhanced the loss of the oriP plasmid in the transient transfection assays.[10,11] In the subacute phase of EBV infection, the establishment of EBV latency was potently blocked by dnE1. In addition, we observed a strong repressive effect of dnE1 on the EBNA1-dependent enhancement of viral gene transcription from C/Wp during the early phase of EBV infection, similar to the transient transfection assays.[17] These data suggest that viral oncogene expression depends heavily on EBNA1 during the acute phase of viral infection, and that EBNA1 contributes little to EBV genome maintenance during this period. The results emphasize that an EBNA1 inhibitor should serve as an attenuator of viral oncogene expression since activation of C/Wp is the 'root' event of the positive feedback loop involved in the transactivation of viral transforming gene expression. In this regard, the EBNA1 inhibition approach could be superior to LMP-1 or EBNA2 inhibition.

If EBNA1 binding to oriP is essential for both the enhancement of viral gene transcription and for genome maintenance, what mechanism prevents dnE1 from affecting the ROL during the acute phase of EBV infection? It is likely that maintenance of the oriP replicon immediately after its introduction into cells is less efficient than in cells harboring an 'established' oriP replicon as an autonomously replicating plasmid. The ROL of an established oriP replicon is 2–4% per cell generation.[10,11] In contrast, our data from the EBV/B cell-based assay gave an average ROL of 26–38% during the week post-infection (acute phase of EBV infection). In agreement with our findings, it is reported that a transiently transduced oriP replicon is lost from cells at 26–37% per cell generation 1–2 weeks post-plasmid transduction.[12] These data indicate that maintenance of the oriP replicon is largely EBNA1-independent immediately after its introduction into cells, regardless of whether the route of introduction is by transfection or EBV infection. In other words, the establishment of EBV latency should be a rare epigenetic event. The data also suggest that the artificial minichromosome approach may be relevant in understanding EBV genome behavior.[12]

Our study suggests that gene therapy using GFP-dnE1 is an attractive approach, not only for therapeutics, but also for prophylactic interventions of EBV-associated malignancies. For example, in peripheral blood stem cell transplantation (PBSCT), GFP-dnE1 transduction into $CD34^+$ cells should protect the differentiated B cells from EBV infection, thus preventing the genesis of EBV-associated B cell lymphomas. We will attempt to prove this hypothesis using a small animal model in future studies.[26] Additionally, EBNA1 is a potential molecular target for developing a small molecular-weight EBV inhibitor as mentioned previously.[14,15] The advantages of EBNA1-inhibitor development are that the biological assay system is already established and the X-ray crystal structure of the DNA-bound EBNA1 DNA binding and dimerization domain is known, which means that computer-aided drug design technology can be immediately applied. Although EBV is associated with various malignancies, preventive and therapeutic measures against EBV infection have not been developed. We believe that an anti-EBV agent, such as an EBNA1 inhibitor, would have an enormous impact in the medical field due to the substantial number of patients with EBV-associated malignancies.

Acknowledgments

We thank Drs Kenichi Imadome and Shigeyoshi Fujiwara for reagents. We also thank Dr Bill Sugden for critically reading the manuscript. This work was supported by the Japan Health Science Foundation, the Ministry of Health, Labor and Welfare of Japan, and the Ministry of Education, Culture, Sports, Science and Technology of Japan.

Disclosure Statement

The authors have no conflict of interest.

References

1 Thompson MP, Kurzrock R. Epstein–Barr virus and cancer. *Clin Cancer Res* 2004; **10**: 803–21.
2 Rickinson AB, Kieff E. Epstin–Barr virus. In: Knipe DM, Howley PM, eds. *Fields Virology*, 5th edn, vol. 2. Philadelphia: Lippincott Williams & Wilkins, 2007; 2655–700.
3 Klein E, Kis LL, Klein G. Epstein–Barr virus infection in humans: from harmless to life endangering virus-lymphocyte interactions. *Oncogene* 2007; **26**: 1297–305.
4 Snow AL, Martinez OM. Epstein–Barr virus: evasive maneuvers in the development of PTLD. *Am J Transplant* 2007; **7**: 271–7.
5 Besson C, Goubar A, Gabarre J *et al.* Changes in AIDS-related lymphoma since the era of highly active antiretroviral therapy. *Blood* 2001; **98**: 2339–44.
6 Carbone A, Cesarman E, Spina M, Gloghini A, Schulz TF. HIV-associated lymphomas and gamma-herpesviruses. *Blood* 2009; **113**: 1213–24.
7 Kieff E, Rickinson AB. Epstin–Barr virus and its replication. In: Knipe DM, Howley PM, eds. *Fields Virology*, 5th edn, vol. 2. Philadelphia: Lippincott Williams & Wilkins, 2007; 2603–54.
8 Lindner SE, Sugden B. The plasmid replicon of Epstein–Barr virus: mechanistic insights into efficient, licensed, extrachromosomal replication in human cells. *Plasmid* 2007; **58**: 1–12.
9 Wang J, Sugden B. Origins of bidirectional replication of Epstein–Barr virus: models for understanding mammalian origins of DNA synthesis. *J Cell Biochem* 2005; **94**: 247–56.
10 Kirchmaier AL, Sugden B. Plasmid maintenance of derivatives of oriP of Epstein–Barr virus. *J Virol* 1995; **69**: 1280–3.
11 Sugden B, Warren N. Plasmid origin of replication of Epstein–Barr virus, oriP, does not limit replication in cis. *Mol Biol Med* 1988; **5**: 85–94.
12 Leight ER, Sugden B. Establishment of an oriP replicon is dependent upon an infrequent, epigenetic event. *Mol Cell Biol* 2001; **21**: 4149–61.
13 Hurley EA, Thorley-Lawson DA. B cell activation and the establishment of Epstein–Barr virus latency. *J Exp Med* 1988; **168**: 2059–75.
14 Altmann M, Pich D, Ruiss R, Wang J, Sugden B, Hammerschmidt W. Transcriptional activation by EBV nuclear antigen 1 is essential for the expression of EBV's transforming genes. *Proc Natl Acad Sci U S A* 2006; **103**: 14188–93.
15 Kennedy G, Komano J, Sugden B. Epstein–Barr virus provides a survival factor to Burkitt's lymphomas. *Proc Natl Acad Sci U S A* 2003; **100**: 14269–74.
16 Nasimuzzaman M, Kuroda M, Dohno S *et al.* Eradication of Epstein–Barr virus episome and associated inhibition of infected tumor cell growth by adenovirus vector-mediated transduction of dominant-negative EBNA1. *Mol Ther* 2005; **11**: 578–90.
17 Kirchmaier AL, Sugden B. Dominant-negative inhibitors of EBNA-1 of Epstein–Barr virus. *J Virol* 1997; **71**: 1766–75.
18 Komano J, Miyauchi K, Matsuda Z, Yamamoto N. Inhibiting the Arp2/3 complex limits infection of both intracellular mature vaccinia virus and primate lentiviruses. *Mol Biol Cell* 2004; **15**: 5197–207.
19 Aiyar A, Sugden B. Fusions between Epstein–Barr viral nuclear antigen-1 of Epstein–Barr virus and the large T-antigen of simian virus 40 replicate their cognate origins. *J Biol Chem* 1998; **273**: 33073–81.
20 Middleton T, Sugden B. EBNA1 can link the enhancer element to the initiator element of the Epstein–Barr virus plasmid origin of DNA replication. *J Virol* 1992; **66**: 489–95.
21 Urano E, Kariya Y, Futahashi Y *et al.* Identification of the P-TEFb complex-interacting domain of Brd4 as an inhibitor of HIV-1 replication by functional cDNA library screening in MT-4 cells. *FEBS Lett* 2008; **582**: 4053–8.
22 Shimizu S, Urano E, Futahashi Y *et al.* Inhibiting lentiviral replication by HEXIM1, a cellular negative regulator of the CDK9/cyclin T complex. *AIDS* 2007; **21**: 575–82.
23 Kanda T, Yajima M, Ahsan N, Tanaka M, Takada K. Production of high-titer Epstein–Barr virus recombinants derived from Akata cells by using a bacterial artificial chromosome system. *J Virol* 2004; **78**: 7004–15.
24 Mackey D, Sugden B. The linking regions of EBNA1 are essential for its support of replication and transcription. *Mol Cell Biol* 1999; **19**: 3349–59.
25 Howe JG, Shu MD. Epstein–Barr virus small RNA (EBER) genes: unique transcription units that combine RNA polymerase II and III promoter elements. *Cell* 1989; **57**: 825–34.
26 Yajima M, Imadome K, Nakagawa A *et al.* A new humanized mouse model of Epstein–Barr virus infection that reproduces persistent infection, lymphoproliferative disorder, and cell-mediated and humoral immune responses. *J Infect Dis* 2008; **198**: 673–82.

doi: 10.1111/j.1349-7006.2009.01474.x

Vaccine 28S (2010) B68–B74

Contents lists available at ScienceDirect

Vaccine

journal homepage: www.elsevier.com/locate/vaccine

T cell-based functional cDNA library screening identified SEC14-like 1a carboxy-terminal domain as a negative regulator of human immunodeficiency virus replication

Emiko Urano[a,b], Reiko Ichikawa[a], Yuko Morikawa[b], Takeshi Yoshida[c], Yoshio Koyanagi[c], Jun Komano[a,*]

[a] National Institute of Infectious Diseases, 1-23-1 Toyama, Shinjuku-ku, Tokyo 162-8640, Japan
[b] Graduate School of Infection Control Sciences, Kitasato University, Shirokane 5-9-1, Minato-ku, Tokyo 108-8641, Japan
[c] Laboratory of Viral Pathogenesis, Institute for Virus Research, Kyoto University, Kyoto 606-8507, Japan

ARTICLE INFO

Article history:
Received 16 May 2009
Received in revised form 7 July 2009
Accepted 24 July 2009

Keywords:
HIV-1
SEC14L1a
Genome-wide screening

ABSTRACT

Genome-wide screening of host factors that regulate HIV-1 replication has been attempted using numerous experimental approaches. However, there has been limited success using T cell-based cDNA library screening to identify genes that regulate HIV-1 replication. We have established a genetic screening strategy using the human T cell line MT-4 and a replication-competent HIV-1. With this system, we identified the C-terminal domain (CTD) of SEC14-like 1a (SEC14L1a) as a novel inhibitor of HIV-1 replication. Our T cell-based cDNA screening system provides an alternative tool for identifying novel regulators of HIV-1 replication.

1. Introduction

The molecular interaction between HIV-1 and the host is not fully understood. A systematic genome-wide approach provides the critical information for the completion of the HIV-1-host interactome. Many experimental genome-wide screening systems have been established to identify the cellular genes required for HIV-1 replication (Table 1, [1–8]). More than a hundred genes have been identified as being cellular factors that regulate HIV-1 replication. However, different screening systems do not identify the same set of genes, and many systems yielded non-overlapping candidates. These discrepancies are assumed to be due to differences in the experimental approaches, such as the virus, the cell line, or the genetic materials used.

For viruses, the wild-type HIV-1 [1,3–6] or a replication-incompetent HIV-1 pseudotyped with vesicular stomatitis virus (VSV)-G is used [2,7,8]. The VSV-G-pseudotyped "HIV-1-based vector" has been used to identify factors associated with the viral entry processes. However, in reality, it covers the events from post-membrane fusion to translation. One of the potential caveats in the use of the VSV-G-pseudotyped vector is that it enters cells via the VSV-G-restricted route, which is fundamentally different from the HIV-1 *Env*-mediated entry pathway [9–12]. The replication-competent HIV-1 should be ideal to cover the entire viral replication cycle; however, this may raise biosafety concerns.

For cells, non-T cells, such as a genetically engineered HeLa cells that ectopically express luciferase or beta-galactosidase (TZM-bl cells), are often used, since they are efficiently transduced with genetic materials [2,5–8]. Not many studies employ a T cell-based system, partly because genetic materials are not efficiently transduced into T cells [1,3,4]. To identify HIV-1 replication regulatory factors, it is preferable to perform the functional analysis in the natural targets of HIV-1 including T cells. The gene expression profile of non-T cells is apparently different from that of T cells as exemplified by the absence of T cell specific markers on non-T cells such as CD4. It is possible that a candidate gene isolated in the non-T cell-based system might not be expressed in T cells. It is impossible to identify T cell-specific factors in the non-T cell-based screening using the siRNA library or in the screening using cDNA libraries derived from non-T cells. Also, the effect or functions of some genes may not be identical in distinct cell types. The potential risk of a non-T cell-based assay is that we may falsely score a gene as a regulator of HIV-1 replication, although many genes have been discovered using non-T cell-based screening systems including the viral receptors. Ideally, the primary CD4-positive T cells, dendritic cells, macrophages, or NK/T cells should be used.

* Corresponding author at: AIDS Research Center, National Institute of Infectious Diseases, 1-23-1 Toyama, Shinjuku, Tokyo 162-8640, Japan. Tel.: +81 3 5285 1111; fax: +81 3 5285 5037.
E-mail address: ajkomano@nih.go.jp (J. Komano).

0264-410X/$ – see front matter © 2009 Elsevier Ltd. All rights reserved.
doi:10.1016/j.vaccine.2009.07.084

Table 1
Summary of genome-wide screening strategies to identify regulatory factors of HIV-1 replication.

Genetic material	Transduction approach	Cell line	Replication competency of HIV-1	Reference
cDNA library	Retroviral, stable	TE671	Incompetent	[2,8]
siRNA library	Transfection, transient	HeLa or 293T	Competent or incompetent	[5,6,7]
cDNA library	Lenti- or retroviral, stable	MT-4	Competent	[1,3,4]

Given technical limitations, this is currently unrealistic for genetic screening experiments.

As for the genetic material, cDNA libraries are often used [1–4,8]. Recent studies utilized siRNA libraries [5–7]. The cDNA approach is advantageous for providing genetic diversity. Expression of the full-length open reading frame of a gene can upregulate the function of the gene, whereas cDNA fragments can function in a diverse fashion. The gene silencing approach downregulates gene expression; however, the silencing efficiency of a gene varies in different cell types and at different time points in the assay (reviewed in [13]). As mentioned above, the gene silencing approach is unable to score the contribution of genes that are not expressed in the cells used in the assay.

The screening can be performed in cells that are either transiently [5–7] or stably [1–4,8] transduced with genetic materials. In the transient transfection assays, it is possible that the dysregulation of a gene function can damage the physiology of the cells. In such a case, the inhibition of HIV-1 replication can be observed, but may not be a direct inhibitory effect of the gene of interest. Such a risk can be minimized by using cells stably transduced with the genetic materials.

We conducted a phenotype cDNA screen using a T cell line-based assay to identify cellular genes that render cells resistant to HIV-1 replication [3]. The advantage of our functional screening system is that cDNA libraries are stably transduced into cells, and that a replication-competent HIV-1 and a human T cell line MT-4 are used. With this system, we have successfully identified the SEC14-like 1a (SEC14L1a) C-terminal domain (CTD) as an inhibitor of HIV-1 replication that targets the late phase of the viral life cycle.

2. Materials and methods

2.1. Cells, transfection, cDNA selection

Cells were maintained in RPMI 1640 medium (Sigma, St. Louis, MA) supplemented with 10% fetal bovine serum (Japan Bioserum, Tokyo, Japan), 100 U/ml penicillin, and 100 μg/ml streptomycin (Invitrogen, Tokyo, Japan). Cells were incubated at 37 °C in a humidified 5% CO_2 atmosphere. Cells were transfected with Lipofectamine 2000 according to the manufacturer's protocol (Invitrogen). The method of selecting human cDNAs that confer resistance to HIV-1 has been described previously in detail [1,3].

2.2. Plasmids

The SEC14L1a CTD1 was amplified from MT-4 polyA RNA by reverse transcriptase PCR (RT-PCR) using the primers 5'-GCACCGGTCTCGAGCCACCATGGACTACAAAGACGATGACGACCCTGCGTGCGCCGCCAGCAGC-3′ and 5'-CCAATTGCTACCTGGAGATCATGGAGCTG-3'. The SEC14L1a CTD2 was amplified by PCR from human lymph node cDNA library (Takara, Otsu, Japan) using the primers 5'-GCACCGGTCTCGAGCCACCATGGACTACAAAGACGATGACGACTGCGAAGTGCCAGAGGGTGGAC-3' and 5'-CCAATTGCTACCTGGAGATCATGGAGCTG-3'. Full length (FL) SEC14L1a was amplified by PCR from a plasmid containing the SEC14L1a open reading frame (ORF, CS0DL004YN18, Invitrogen), using the primers 5'-GCACCGGTCTCGAGCCACCATGGACTACAAAGACGATGACGACGTGCAGAAATACCAGTCCCCAG-3' and 5'-CCAATTGCTACCTGGAGATCATGGAGCTG-3'. The AgeI-MfeI fragments of the PCR products were cloned into the XmaI-MfeI sites of the pEGFP-C3 plasmid (Clontech, Palo Alto, CA), generating pEGFP-SEC14L1a-CTD1, -CTD2, and -FL. The XhoI-MfeI fragments from the resulting plasmids were cloned into the corresponding restriction sites of the pCMMP KRAB vector, creating pCMMP GFP-SEC14L1a-CTD1, -CTD2, and -FL. The HIV-1 *tat* was amplified by PCR using the primers 5′-AACCGGTCTCGAGCCACCATGGAGCCAGTAGATCCTAGAC-3′ and 5′-GGATCCTCAGTCGTCATCGTCTTTGTAGTCTTCCTTCGGGCCTGTCGGGTC-3′. A Tat expression vector pCMMP Tat was constructed by cloning the AgeI-BamHI fragment of the PCR product into the corresponding restriction sites of the pCMMP KRAB vector. The HIV-1 *Env* and GFP expression vectors (pIIIex and pCMMP GFP, respectively) are described previously [3,12,14]. To construct the pCMMP GFP-FLAG (GFPf), pCMMP CXCR4 d-10 [15] was digested with AgeI and XhoI to remove CXCR4 d-10 ORF and self-ligated after blunting with T4 DNA polymerase. The HIV-1 *gag-pol*, *tat*, and *rev* expressing plasmid pCMVR8.91 was a generous gift from Dr. Trono's group [16].

2.3. Western blotting

Western blotting was performed according to techniques described previously [17]. The following reagents were used: anti-FLAG (rabbit polyconal, 600-401-383, Rockland, Gilbertsville, PA), anti-p24 (183-H12-5C, NIH AIDS Research and Reference Reagent Program), anti-gp120 (vA-20 and vT-21 antibodies, Santa Cruz Biotech, Santa Cruz, CA), biotinylated anti-goat antibody (GE Healthcare Bio-Sciences, Piscataway, NJ), horseradish peroxidase-conjugated streptoavidin (GE Healthcare Bio-Sciences), and EnVision+ system (Dako, Glostrup, Denmark). Signals were visualized with an LAS3000 imager (Fujifilm, Tokyo, Japan) and quantified by Multi Gauge ver 3.0 software (Fujifilm).

2.4. Confocal microscopy

293T cells transiently transfected with expression vectors for SEC14L1a derivatives were grown on glass plates, fixed in 4% formaldehyde in phosphate buffer saline (PBS) for 5 min at 24 h post-transfection, stained with Hoechst 33258 (Sigma), mounted (Vectorshield, Vector Laboratories, Burlingame, CA), and imaged using a confocal microscope META 510 (Carl Zeiss, Tokyo, Japan). For MT-4 cells, live cells were incubated with Hoechst 33258 and imaged unfixed. Image brightness and contrast were processed by META510 software (Carl Zeiss).

2.5. Immunoprecipitation

Cells expressing FLAG-tagged proteins were harvested and washed twice with PBS and then lysed in the lysis buffer (50 mM Tris–HCl, pH 8.0, 0.5% IGEPAL CA630, protease inhibitor cocktail from Sigma) on ice for 30 min. The soluble fraction was obtained by centrifugation at 15,000 rpm for 30 min at 4 °C, and was incubated with 20 μl of Red-Anti-FLAG M2 Affinity Gel (Sigma) with gentle mixing overnight at 4 °C. After washing the agarose beads for five times with the lysis buffer, the bound complexes were eluted with the FLAG peptide, and analyzed by Western blotting.

2.6. Flow cytometry

Cells were labeled with PE-Cy5-conjugated anti-CD4 antibody or PE-conjugated anti-CXCR4 antibody (Beckton Dickinson, San Jose, Calif.) for 30 min at 4 °C. Cells were washed once with PBS supplemented with 1% FBS and analyzed by FACS Aria (Beckton Dickinson). The GFP-positive cells were sorted using FACS Aria.

2.7. Monitoring HIV-1 replication

For HIV-1 infection, 1×10^5 cells were incubated at the room temperature with the HIV-1_{HXB2}-containing culture supernatant, which had approximately 1.0 ng of $p24^{CA}$, for approximately 30 min. The culture supernatants were collected at 4 d post-infection and subjected to ELISA to measure the $p24^{CA}$ antigen, using a Retro TEK p24 Antigen ELISA Kit according to the manufacturer's protocol (Zepto Metrix, Buffalo, NY). The signals were measured with an ELx808 microplate photometer (BIO-TEK®, Winooski, VT).

2.8. PCR analysis

The cellular DNA and RNA were extracted from cells infected with VSV-G-pseudotyped HIV-1 vector produced by using pNL-Luc plasmid, as described previously [17]. The Alu-LTR PCR and RT-PCR were performed as described previously [3,17] using the following primers: for the first Alu-LTR PCR reaction, 5'-AACTAGGGAACCCACTGCTTAAG-3' and 5'-TGCTGGGATTACAGGC-GTGAG-3'; and for the second Alu-LTR PCR reaction, 5'-AACT-AGGGAACCCACTGCTTAAG-3' and 5'-CTGCTAGAGATTTTCCACA-CTGAC-3'. For amplification of HIV-1 mRNA, 5′-ATGGAGCCAGTAG-ATCCTAGAC-3′ and 5′-CTATTCCTTCGGGCCTGTCGGG-3′ primers were used. For the control, we amplified beta-globin and cyclophilin A using the following primers: beta-globin, 5'-TATTGGTCT-CCTTAAACCTGTCTTG-3' and 5'-CTGACACAACTGTGTTCACTAGC-3'; and cyclophilin A, 5′- CACCGCCACCATGGTCAACCCCACCGTGTTCT-TCGAC-3′ and 5′- CCCGGGCCTCGAGCTTTCGAGTTGTCCACAGTCA-GCAATGG-3′. The amplicons were separated in a 2% agarose gel, stained with ethidium bromide, and imaged with a Typhoon scanner (GE Healthcare Bio-Sciences).

2.9. Collection of virus-like particle

Tissue culture supernatants containing virus-like particles (VLP) were passed through nitrocellulose filters (0.45 μm, Millipore, Tokyo, Japan) and the virions were collected by centrifugation (Optima™ TL, TLA 100.3 rotor, 541 k × *g* for 1 h; Beckman Coulter, Miami, FL).

3. Results

3.1. Identification of SEC14L1a as a potential regulator of HIV-1 replication

We prepared MT-4 cells that constitutively express cDNA transduced by a lentiviral vector or an MLV-based retroviral vector (Fig. 1A). The cDNAs were derived from human peripheral blood mononuclear cells (PBL) and *Oryctolagus cuniculus* (European rabbit) kidney-derived cell line RK13 cells. MT-4 cells transduced with cDNA were collected by FACS sorter using the green fluorescence as a marker since viral vectors encoded the GFP expression cassette. Then, cells were infected with HIV-1. Surviving cells were propagated and the genomic DNA was extracted to recover the transduced cDNA by PCR as previously described [3]. We isolated two clones encoding the carboxy terminal domain (CTD) of SEC14L1a (Gene ID 6397, Fig. 1B and C); one from the PBL cDNA library (1/65 independent clones, 1.5%), and one from the RK13 cDNA library (1/42 independent clones, 2.4%). The fact that the SEC14L1a CTD was successfully identified from two independent cDNA libraries strongly suggests that it is a negative regulator of HIV-1 replication. It is important to note that previous genome-wide screenings for HIV-1 regulators have not identified SEC14L1a CTD. This clearly suggests that our T cell-based cDNA screening system is unique, and should be able to complement the other genome-wide screening systems.

SEC14L1a belongs to the widely-expressed SEC14-superfamily that is involved in membrane trafficking and phospholipid metabolism [18–21]. The function of SEC14L1a is not well understood. The C-terminus of SEC14L1a encodes a Golgi dynamics (GOLD) domain (amino acids (aa) 523–674; Fig. 1C) that mediates the protein-protein interaction possibly involved in the maintenance of Golgi apparatus function and vesicular trafficking [22]. The only reported biological activity of SEC14L1a is to interact with cholinergic receptors AchT and CHT1 [23]. The GOLD domain is responsible for the physical interaction between SEC14L1a and cholinergic receptors. However, the functional significance of these interactions remains to be clarified. The conserved SEC14 domain directly interacts with lipid molecules [17–21]. However, the lipid ligand of SEC14L1a (aa 319–490, Fig. 1C) has yet to be identified.

3.2. Construction of expression vectors for SEC14L1a derivatives

The longest SEC14L1a cDNA recovered from the PBL cDNA library spanned nucleotides (nt) 2045–2492 of SEC14L1a mRNA (NM_003003.3), covering the CTD of the SEC14L1a open reading frame (ORF; Fig. 1B). We detected a potential translational start codon at nt 2188-2190 within the GOLD domain (asterisk, Fig. 1B). We speculated that the isolated cDNA might have expressed the carboxy half of the GOLD domain (aa 641–715) in MT-4 cells, leading to the inhibition of HIV-1 replication.

To test this, we constructed an expression plasmid for FLAG-tagged CTD (aa 642-715) fused to the carboxy terminus of GFP (CTD1; Fig. 1C). We also constructed GFP fusion proteins spanning the GOLD domain (CTD2, aa 493–715) or the full-length SEC14L1a (FL; Fig. 1C). Expression of these proteins was verified by Western blotting of transient transfected 293T cells (Fig. 1D). The confocal microscopy analysis indicated that the FL localized mainly in the cytoplasm, with some accumulation in the perinuclear regions (Fig. 1E), consistent with a previous report [23]. CTD1 was distributed in the cytoplasm and the nucleus, with a slight preference for the cytoplasm. CTD2 was evenly distributed to the nucleus and cytoplasm. When MT-4 cells constitutively expressing FL, CTD1, and CTD2 were analyzed, the subcellular distribution was less clear, due to the small cytoplasm (Fig. 1F). However, FL was distributed evenly to the nucleus and cytoplasm in MT-4 cells. In contrast, CTD1 was excluded from the nucleus in MT-4 cells (Fig. 1F). The distribution of CTD2 in MT-4 cells was similar to that in 293T cells (Fig. 1F). The differences of protein distribution in two cell types may be caused by the cell type-dependent regulation of protein trafficking and/or the effect of protein expression levels.

3.3. Verification of anti-HIV-1 activity associated with SEC14L1a CTD1

We introduced FL, CTD1, or CTD2 into MT-4 cells using the MLV vector, and isolated cells constitutively expressing FL, CTD1, or CTD2. Expression of SEC14L1a derivatives in MT-4 cells was verified by Western blotting (Fig. 2A). FL expression was verified by immuno-precipitation assay (Fig. 2A). The detection of FL by Western blotting was inefficient considering the fact that all the SEC14L1a derivatives are GFP-tagged, and the GFP intensity of FL-expressing MT-4 cells was not lower than that of CTD1-expressing

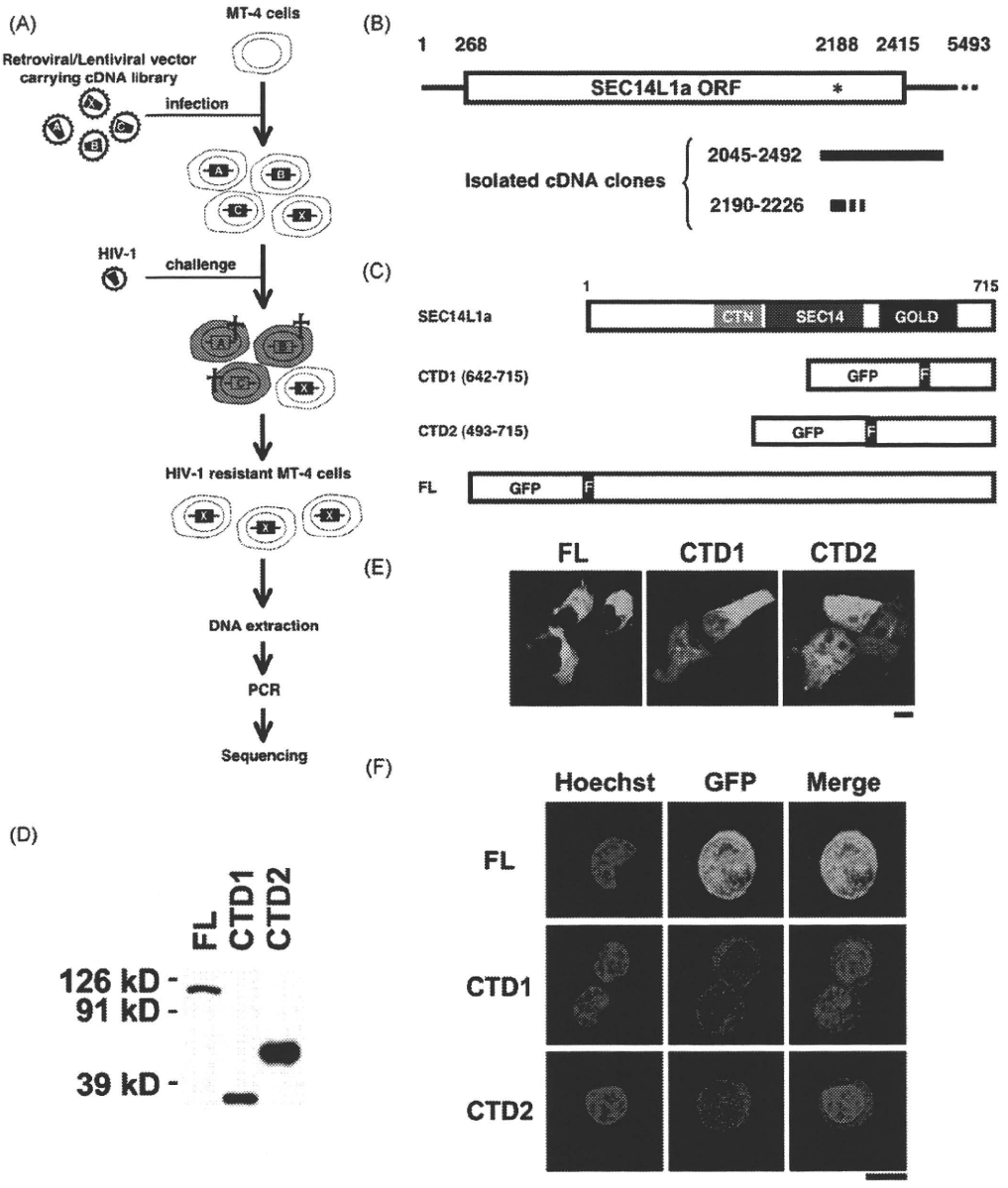

Fig. 1. Identification of SEC14L1a CTD as a potential regulator of HIV-1 replication. (A) The experimental strategy used to screen a cDNA library for genes rendering cells resistant to HIV-1. MT-4 cells were infected with a retroviral or lentiviral vector carrying cDNA libraries and were challenged with wild-type HIV-1_{HXB2}. The HIV-1-infected cells (gray with cross) quickly undergo cell death. The surviving cells were propagated, collected, and the transduced cDNA labeled X was determined. (B) Schematic representation of SEC14L1a mRNA (NM_00303.3) and the isolated gene fragments. The open reading frame (ORF) is assigned from nucleotides (nt) 268 to 2415. The potential internal translational initiation codon is marked with an asterisk. (C) Schematic representation of the SEC14L1a protein (NP_002994). SEC14L1a has a CRAL_TRIO_N domain (CTN, amino acids 241–313), a SEC14p-like lipid-binding domain (SEC14, amino acids 319–490), and a Golgi dynamics domain (GOLD, amino acids 523–674). The cloned fragments (CTD1 and CTD2) and full-length (FL) gene were tagged with a FLAG epitope (indicated with an "F") on their N-termini, and fused to the C-terminus of GFP. (D) Verification of FL, CTD1, and CTD2 expression in 293T cells by Western blotting using anti-FLAG antibody. (E) Confocal microscopy images of 293T cells expressing FL, CTD1, or CTD2. The green signal represents GFP fluorescence. Magnification, 630×; scale bar, 10 μm. (F) Confocal microscopy images of MT-4 cells constitutively expressing FL, CTD1, or CTD2. The blue signal represents the Hoechst-stained nucleus, and green represents GFP fluorescence. Magnification, 630×; scale bar, 5 μm.

cells (Fig. 1F). The MLV vector expressing GFP alone was used as a control. The cell proliferation, morphology, and cell surface levels of HIV-1 receptors were unaltered by any of the SEC14L1a derivatives (Fig. 1F, 2B, and data not shown). HIV-1 replication was tested in these cells. The level of HIV-1 replication was significantly inhibited in CTD1- and CTD2-expressing cells (69.1% and 69.8% on the average from seven independent experiments, respectively, $P < 0.05$, two-tailed Student's *t*-test), but was hardly inhibited in FL-expressing cells (86.4%, not statistically significant; Fig. 2C). This observation was reproducible in independently established MT-4 cells and SupT1 cells (data not shown). These data verified the original screening results, and suggest that the C-terminal half of GOLD domain of SEC14L1a serves as an inhibitor of HIV-1 replication. In contrast, it is suggested that FL is not a potent negative regulator of HIV-1 replication.

3.4. SEC14L1a CTD1 and CTD2 target the late phase of the HIV-1 life cycle

We analyzed the viral entry and production phases to determine which step of the HIV-1 life cycle CTD1 and CTD2 target.

The Alu-LTR PCR assay was performed to examine the effect of SEC14L1a derivatives on the viral entry phase. The MT-4 cells stably expressing GFP, FL, CTD1, or CTD2 were infected with VSV-

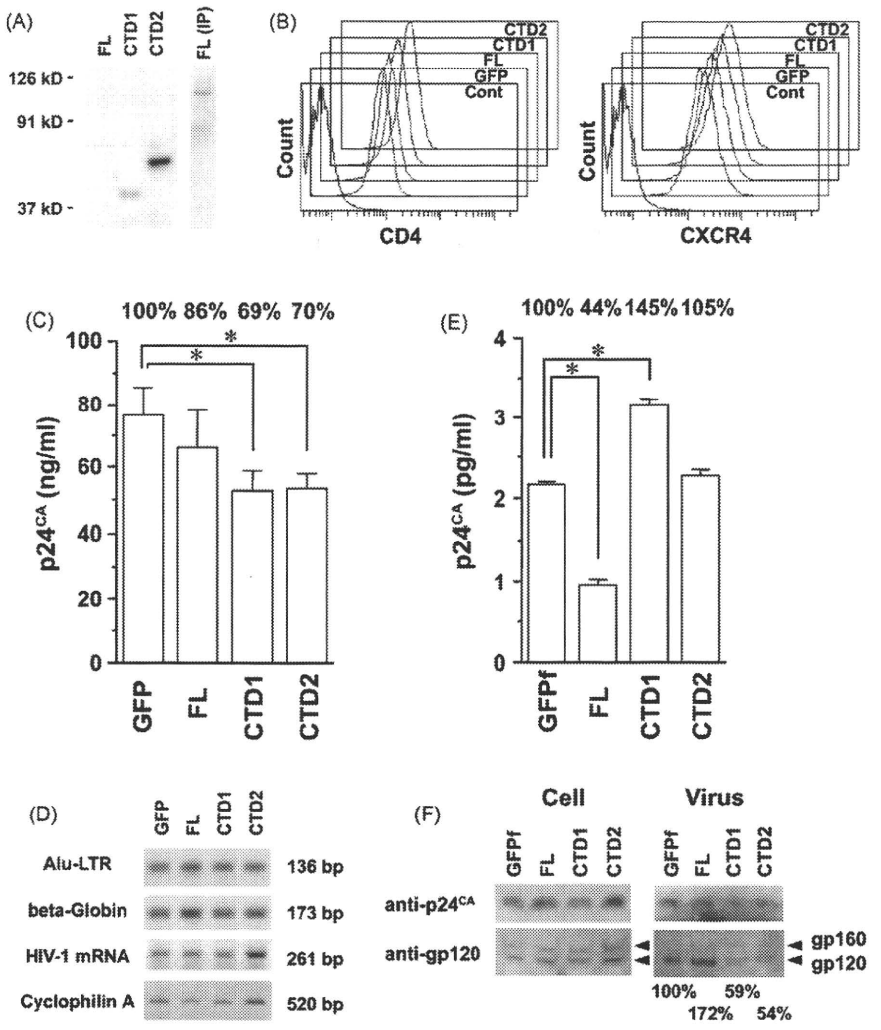

Fig. 2. Functional characterization of the SEC14L1a derivatives. (A) Detection of stable expression of FL, CTD1, and CTD2 in MT-4 cells by Western blotting using anti-FLAG antibody. FL was detected by the immunoprecipitation (IP) assay using agarose beads conjugated with anti-FLAG antibody. The flow cytometric analysis of the cell surface expression of HIV-1 receptors CD4 and CXCR4 in MT-4 cells stably expressing GFP, FL, CTD1, and CTD2. (C) Constitutive expression of CTD1 and CTD2 limited the replication of HIV-1 in MT-4 cells. The concentration of viral $p24^{CA}$ antigen in the culture supernatant was measured at 4 d post-infection. The results represent the average of seven independent experiments ± the standard error of the mean. The reduction of viral $p24^{CA}$ concentration relative to GFP was shown on the top. Asterisks indicate the statistical significance compared to GFP ($P<0.05$ by two-tailed Student's *t*-test). (D) The PCR-based assay to examine the effect of SEC14L1a derivatives on the early phase of viral life cycle (top two panels) and the transcription from LTR promoter (bottom two panels). The HIV-1 entry efficiency was examined by Alu-LTR PCR. Beta globin was used as an internal control. The HIV-1 transcription efficiency was examined by RT-PCR targeting spliced viral mRNA. Cyclophilin A was used as a control. The expected length of each PCR amplicon was indicated. (E) The effect of SEC14L1a derivatives on the HIV-1 production. The 293T cells grown in a well of a 6-well plate were transfected with 200 ng of HIV-1 proviral DNA and 2 μg of expression vector for GFPf, FL, CTD1, or CTD2. The culture supernatant was recovered at 2 d post-transfection and the $p24^{CA}$ concentration was measured. The representative data from five independent experiments was shown. The results indicate the average ± the standard deviation. The relative $p24^{CA}$ concentration compared to GFPf was shown on the top. Asterisks indicate the statistical significance compared to GFPf ($P<0.001$ by two-tailed Student's *t*-test). The *Env* incorporation onto the virus-like particles (VLP) produced by 293T cells expressing SEC14L1a derivatives. The 293T cells grown in a well of a 6-well plate were transfected with 1 μg of *gag-pol* (pCMVR8.91) and *Env* (pIIIex) expression vectors along with 2 μg of expression vector for GFPf, FL, CTD1, or CTD2. The cell lysates (Cell) and VLP fractions (Virus) were subjected to Western blot analysis detecting gp120 and $p24^{CA}$ harvested at 2 d post-transfection. The *Env* incorporation levels normalized to $p24^{CA}$ relative to GFPf were shown at the bottom.

G-pseudotyped HIV-1 vector, and the cellular genomic DNA was recovered at 4 d post-infection. The amount of Alu-LTR PCR products from FL-, CTD1-, or CTD2-expressing MT-4 cells was almost equal to that from GFP-expressing cells, suggesting that the early phase of the viral life cycle is not inhibited by any of the SEC14L1a derivatives (Fig. 2D). To examine the viral production phase, we examined the LTR-driven viral gene transcription by RT-PCR. Cellular RNA was extracted from the same MT-4 cells infected with VSV-G-pseudotyped HIV-1 vector, and RT-PCR was conducted to amplify LTR promoter-driven spliced HIV-1 mRNA. The amount of viral RNA expressed in FL-, CTD1-, or CTD2-expressing cells was not lower than that in GFP-expressing cells when the levels of the internal control was taken into account (Fig. 2D). Given that the similar number of viral genome was integrated as indicated by the Alu-LTR PCR, these data suggest that viral transcription is not inhibited by any of the SEC14L1a derivatives, and that the action point of CTD1 and CTD2 should be at post-transcriptional levels of the viral production phase.

Next, the FL, CTD1, or CTD2 expression vector was co-transfected with HIV-1 proviral DNA into 293T cells, and viral production was quantified by $p24^{CA}$ ELISA. The FLAG-tagged GFP (GFPf) was used as a control hereafter. We found that the FL expression significantly reduced the production of HIV-1 (44.2%, $P<0.001$, two-tailed Student's *t*-test) compared to the GFPf control (Fig. 2E). In contrast, the CTD1 enhanced the production of HIV-1 (145.9%, $P<0.001$, two-tailed Student's *t*-test; Fig. 2E). However, CTD2 did not measurably affect the HIV-1 production (105.1%, not statistically significant; Fig. 2E). As the ELISA assay examines the effect

of CTDs on *Gag* functions, we next tested the functional interaction between CTDs and *Env*. The *Env* incorporation onto the virion was examined by tripartite-transfection of expression vectors for *Env*, *gag-pol*, and SEC14L1a derivatives into 293T cells, and the VLP was collected by centrifugation. The immunoblotting against gp120 was performed on the cell lysate and the VLP fraction. The cellular *Env* and *Gag* expressions were not detectably affected by any of the SEC14L1a derivatives (Fig. 2F, left panel). The *Env* incorporation onto the VLP was slightly enhanced by FL (157%; Fig. 2F, right panel). In contrast, the VLP produced from CTD1- or CTD2-expressing cells incorporated substantially fewer *Env* than those from GFPf-expressing cells (59% or 54%, respectively; Fig. 2F, right panel). These data were reproducible in independently performed experiments. The densitometric analysis of Western blot image showed that the average ± the standard error of the mean of Env incorporation onto the virion was 129.7 ± 39.9%, 54.8 ± 24.7%, and 25.5 ± 10.3% for FL, CTD1, and CTD2 compared to GFPf, respectively (3–4 independent experiments). The *Env*-mediated cell-to-cell fusion assay indicated that SEC14L1a derivatives did not limit the cell surface targeting and function of *Env* (data not shown). In addition, the *Gag* processing in virion was unaffected by any of the SEC14L1a derivatives (data not shown). Collectively, these data suggest that the HIV-1 replication is inhibited by CTD1 and CTD2 due to the inefficient *Env* incorporation onto the virion. To test this possibility, we infected fresh MT-4 cells with the equal amount of HIV-1 propagated in CTD1- or CTD2-expressing MT-4 cells (1–2 ng $p24^{CA}$), and the viral replication was monitored at 3–4 days post-infection by measuring the $p24^{CA}$ concentration. The infectivity of HIV-1 propagated in CTD1- or CTD2-expressing cells was attenuated to 83.1 ± 17.9% or 82.4 ± 5.5% relative to the virus recovered from GFP-expressing cells, respectively (the average ± the standard error of the mean of 3 independent experiments). Altogether, these data suggest that the inhibition of HIV-1 replication by CTD1 and CTD2 is attributed to the attenuation of viral infectivity by lowering the *Env* incorporation onto the virion.

4. Discussion

In the present study, we provide the first evidence that the C-terminal fragment of SEC14L1a functions as an inhibitor of HIV-1 replication. The advantage of this system is that, since MT-4 cells are stably transduced with a cDNA library, the anti-HIV-1 function of a candidate gene is not due to a perturbed cell physiology. This system has been successful in identifying CD14, CD63, and Brd4-CTD as regulators of HIV-1 replication [1,3,4], and more candidates are being analyzed. Among the candidates, SEC14L1a CTD appeared to be one of the relatively modest inhibitors of HIV-1 replication. However, of note, the SEC14L1a derivatives have not been identified in other genetic screening systems. These facts point that our T cell-based system is sensitive in detecting the modest anti-HIV-1 activity of a gene, and is a unique tool in the pursuit of HIV-1 regulatory factors to complete the HIV-1-host interactome.

SEC14L1a may affect the Golgi-mediated vesicular trafficking since SEC14L1a lowers the cell surface levels of cholinergic transporters [23]. However, we do not have any data to suggest that SEC14L1a and its derivatives affect the cell surface targeting of membrane proteins including CD4, CXCR4 and *Env*. These data suggest that SEC14L1a's effect on cholinergic receptor expression is specific, and that the CTD's ability to inhibit HIV-1 replication is independent from SEC14L1a's regulatory functions on vesicular trafficking. The action point of CTD1 and CTD2 was shown to be the late phase of the viral life cycle. Given that CTD1 and CTD2 did not inhibit the biogenesis and the cell surface targeting of *Gag* and *Env*, the major mechanism of CTD1 and CTD2 to inhibit HIV-1 replication was to reduce the infectivity of HIV-1 by limiting the *Env* incorporation onto the virion. Consistent with this idea, the viral infectivity of virions produced in CTDs-expressing cells was attenuated. Then, how do CTDs block the *Env* incorporation onto the virion? We detected a weak interaction between *Gag* and CTD1 or CTD2 by immuno-coprecipitation analysis. Thus, we speculate that the interaction between *Env* and *Gag* at the plasma membrane is interfered by *Gag*-CTDs interaction, resulting in the reduction of *Env* incorporation onto the virion.

The CTD1 was an inhibitor of HIV-1 replication. While the CTD1 negatively affected the *Env* incorporation onto the virion, it positively affected the HIV-1 production. These observations may be seemingly controversial. However, the SEC14L1a derivatives' effect on HIV-1 replication is a summation of their effects of on each step of the viral life cycle. Therefore, it is conceivable that CTD1 can serve as a negative regulator of HIV-1 replication as well as a positive and negative factor on distinct steps of the viral life cycle. These seemingly controversial findings may be in part due to the cells in which the biological functions of SEC14L1a derivatives were examined. The effect of SEC14L1a derivatives on HIV-1 replication was investigated in MT-4 cells, whereas those on the HIV-1 production and *Env* incorporation onto the virion were examined in 293T cells. Although the basic biological features are largely shared among different cell types, it is possible that the SEC14L1a derivatives may function slightly differently in MT-4 cells from 293T cells given that the intracellular distribution of SEC14L1a derivatives in MT-4 cells was not identical to that in 293T cells (Fig. 1E and 1F).

Elucidating the molecular mechanism underlying CTDs' activity not only provides a hint to understand how the HIV-1 virion actively uptakes *Env* through the *Gag-Env* interaction, but also leads to the development of a novel anti-retroviral drug that lowers the infectivity of the virus by preventing *Env* incorporation onto the virion. This is the strength of our T cell-based assay since CTDs inhibit HIV-1 replication specifically. In the previous study, we proposed that a small portion of Brd4 may serve as a therapeutic molecular target for HIV-1 infection, since the constitutive expression of Brd4-CTD limited HIV-1 replication specifically [3], akin to the SEC14L1a CTDs. However, it remains to be examined whether the SEC14L1a and Brd4 derivatives inhibit HIV-1 replication in primary HIV-1 target cells.

The genome-wide screening has potential caveats, including a cDNA bias and a cell line bias. A cDNA library is not a perfect representation of mRNA expressed in the cells from which the library is constructed. For example, the longer the mRNA, the less efficiently the full-length cDNA is synthesized. In fact, we isolated Brd4-CTD from the PBL cDNA library as a potent inhibitor of HIV-1 replication [3]. However, although Brd4 (approximately 5000 nt mRNA in length) is expressed in MT-4 cells, we were unable to recover Brd4-CTD from the MT-4 cDNA library [3]. This clearly demonstrates the cDNA bias in the genetic screening. A cDNA library derived from non-T cells does not contain genes specifically expressed in T cells. Thus, we have to explore many more cDNA libraries to completely cover the genetic diversity of human cells. The cDNA libraries isolated from long-term non-progressors of HIV-1-seropositive individuals or from elite controllers might be of particular interest, considering that a dominant innate HIV-1 resistance gene, such as CCR5 delta 32, may partly account for the slow progression of AIDS. Similarly, use of a particular cell line and/or virus strain may bias the results. MT-4 cells are positive for HTLV-1, and are able to support robust HIV-1 replication. MT-4 cells do not express CCR5, and are unable to support R5-tropic HIV-1 strains. What if other T cell lines and R5-tropic viral strains are used? What if we assay the same cDNA library in TZM-bl cells? We plan to address these issues in the future studies.

In conclusion, genome-wide genetic screening is a powerful tool for identifying the regulatory factors of HIV-1 replication and innate HIV-1 resistance factors that limit HIV-1 infection and AIDS progression. The HIV-1-host interactome should also reveal poten-

tial therapeutic molecular targets that may be used to develop novel anti-AIDS drugs to tackle the emerging drug resistant viruses. However, the fact that different experimental systems often yield non-overlapping candidates suggests that we have to explore more experimental systems to fully understand the HIV-1-host interactome. Our T cell-based system provides an alternative tool for identifying novel HIV-1 regulatory factors, and should help us understand the HIV-1-host interaction in more detail.

Acknowledgements

This work was supported by the Japan Health Science Foundation, the Japanese Ministry of Health, Labor and Welfare, and the Japanese Ministry of Education, Culture, Sports, Science and Technology.

Conflict of interest statement

The authors state that they have no conflict of interest.

References

[1] Kawano Y, Yoshida T, Hieda K, Aoki J, Miyoshi H, Koyanagi Y. A lentiviral cDNA library employing lambda recombination used to clone an inhibitor of human immunodeficiency virus type 1-induced cell death. J Virol 2004;78(20):11352–9.
[2] Valente ST, Goff SP. Inhibition of HIV-1 gene expression by a fragment of hnRNP U. Mol Cell 2006;23(4):597–605.
[3] Urano E, Kariya Y, Futahashi Y, Ichikawa R, Hamatake M, Fukazawa H, et al. Identification of the P-TEFb complex-interacting domain of Brd4 as an inhibitor of HIV-1 replication by functional cDNA library screening in MT-4 cells. FEBS Lett 2008;582(29):4053–8.
[4] Yoshida T, Kawano Y, Sato K, Ando Y, Aoki J, Miura Y, et al. A CD63 mutant inhibits T-cell tropic human immunodeficiency virus type 1 entry by disrupting CXCR4 trafficking to the plasma membrane. Traffic 2008;9(4):540–58.
[5] Zhou H, Xu M, Huang Q, Gates AT, Zhang XD, Castle JC, et al. Genome-scale RNAi screen for host factors required for HIV replication. Cell Host Microbe 2008;4(5):495–504.
[6] Brass AL, Dykxhoorn DM, Benita Y, Yan N, Engelman A, Xavier RJ, et al. Identification of host proteins required for HIV infection through a functional genomic screen. Science 2008;319(5865):921–6.
[7] Konig R, Zhou Y, Elleder D, Diamond TL, Bonamy GM, Irelan JT, et al. Global analysis of host-pathogen interactions that regulate early-stage HIV-1 replication. Cell 2008;135(1):49–60.
[8] Valente ST, Gilmartin GM, Mott C, Falkard B, Goff SP. Inhibition of HIV-1 replication by eIF3f. Proc Natl Acad Sci USA 2009;106(11):4071–8.
[9] Aiken C. Pseudotyping human immunodeficiency virus type 1 (HIV-1) by the glycoprotein of vesicular stomatitis virus targets HIV-1 entry to an endocytic pathway and suppresses both the requirement for Nef and the sensitivity to cyclosporin A. J Virol 1997;71(8):5871–7.
[10] Akari H, Uchiyama T, Fukumori T, Iida S, Koyama AH, Adachi A. Pseudotyping human immunodeficiency virus type 1 by vesicular stomatitis virus G protein does not reduce the cell-dependent requirement of vif for optimal infectivity: functional difference between Vif and Nef. J Gen Virol 1999;80(Pt 11):2945–9.
[11] Chazal N, Singer G, Aiken C, Hammarskjold ML, Rekosh D. Human immunodeficiency virus type 1 particles pseudotyped with envelope proteins that fuse at low pH no longer require Nef for optimal infectivity. J Virol 2001;75(8):4014–8.
[12] Komano J, Miyauchi K, Matsuda Z, Yamamoto N. Inhibiting the Arp2/3 complex limits infection of both intracellular mature vaccinia virus and primate lentiviruses. Mol Biol Cell 2004;15(12):5197–207.
[13] Goff SP. Knockdown screens to knockout HIV-1. Cell 2008;135(3):417–20.
[14] Urano E, Aoki T, Futahashi Y, Murakami T, Morikawa Y, Yamamoto N, et al. Substitution of the myristoylation signal of human immunodeficiency virus type 1 Pr55Gag with the phospholipase C-delta1 pleckstrin homology domain results in infectious pseudovirion production. J Gen Virol 2008;89(Pt 12):3144–9.
[15] Futahashi Y, Komano J, Urano E, Aoki T, Hamatake M, Miyauchi K, et al. Separate elements are required for ligand-dependent and-independent internalization of metastatic potentiator CXCR4. Cancer Sci 2007;98(3):373–9.
[16] Zufferey R, Dull T, Mandel RJ, Bukovsky A, Quiroz D, Naldini L, et al. Self-inactivating lentivirus vector for safe and efficient in vivo gene delivery. J Virol 1998;72(12):9873–80.
[17] Shimizu S, Urano E, Futahashi Y, Miyauchi K, Isogai M, Matsuda Z, et al. Inhibiting lentiviral replication by HEXIM1, a cellular negative regulator of the CDK9/cyclin T complex. AIDS 2007;21(5):575–82.
[18] Chinen K, Takahashi E, Nakamura Y. Isolation and mapping of a human gene (SEC14L), partially homologous to yeast SEC14, that contains a variable number of tandem repeats (VNTR) site in its 3' untranslated region. Cytogenet Cell Genet 1996;73(3):218–23.
[19] Howe AG, McMaster CR. Regulation of phosphatidylcholine homeostasis by Sec14. Can J Physiol Pharmacol 2006;84(1):29–38.
[20] Saito K, Tautz L, Mustelin T. The lipid-binding SEC14 domain. Biochim Biophys Acta 2007;1771(6):719–26.
[21] Mousley CJ, Tyeryar KR, Vincent-Pope P, Bankaitis VA. The Sec14-superfamily and the regulatory interface between phospholipid metabolism and membrane trafficking. Biochim Biophys Acta 2007;1771(6):727–36.
[22] Anantharaman V, Aravind L. The GOLD domain, a novel protein module involved in Golgi function and secretion. Genome Biol 2002;3(5), research0023.0021-0023.0027.
[23] Ribeiro FM, Ferreira LT, Marion S, Fontes S, Gomez M, Ferguson SS, et al. SEC14-like protein 1 interacts with cholinergic transporters. Neurochem Int 2007;50(2):356–64.

Journal of Medical Virology 82:128–137 (2010)

Induction of Cross-Protective Immunity Against Influenza A Virus H5N1 by an Intranasal Vaccine With Extracts of Mushroom Mycelia

Takeshi Ichinohe,[1,2] Akira Ainai,[1,3] Tomoyuki Nakamura,[4] Yukihito Akiyama,[4] Jun-ichi Maeyama,[5] Takato Odagiri,[3] Masato Tashiro,[3] Hidehiro Takahashi,[1] Hirofumi Sawa,[6] Shin-ichi Tamura,[1] Joe Chiba,[2] Takeshi Kurata,[1] Tetsutaro Sata,[1] and Hideki Hasegawa[1,3]*

[1]*Department of Pathology, National Institute of Infectious Diseases, Musashimurayama-shi, Tokyo, Japan*
[2]*Department of Biological Science and Technology, Tokyo University of Science, Noda-shi, Chiba, Japan*
[3]*Center for Influenza virus Research, National Institute of Infectious Diseases, Musashimurayama-shi, Tokyo, Japan*
[4]*Applied Fungi Institute IBI Corporation, Yamanashi, Japan*
[5]*Department of Safety Research on Blood and Biological Products, National Institute of Infectious Diseases, Musashimurayama-shi, Tokyo, Japan*
[6]*Department of Molecular Pathobiology, 21st Century COE Program for Zoonosis Control, Hokkaido University Research Center for Zoonosis Control, Kita-ku, Sapporo, Japan*

The identification of a safe and effective adjuvant that is able to enhance mucosal immune responses is necessary for the development of an efficient inactivated intranasal influenza vaccine. The present study demonstrated the effectiveness of extracts of mycelia derived from edible mushrooms as adjuvants for intranasal influenza vaccine. The adjuvant effect of extracts of mycelia was examined by intranasal co-administration of the extracts and inactivated A/PR8 (H1N1) influenza virus hemagglutinin (HA) vaccine in BALB/c mice. The inactivated vaccine in combination with mycelial extracts induced a high anti-A/PR8 HA-specific IgA and IgG response in nasal washings and serum, respectively. Virus-specific cytotoxic T-lymphocyte responses were also induced by administration of the vaccine with extract of mycelia, resulting in protection against lethal lung infection with influenza virus A/PR8. In addition, intranasal administration of NIBRG14 vaccine derived from the influenza A/Vietnam/1194/2004 (H5N1) virus strain administered in conjunction with mycelial extracts from *Phellinus linteus* conferred cross-protection against heterologous influenza A/Indonesia/6/2005 virus challenge in the nasal infection model. In addition, mycelial extracts induced proinflammatory cytokines and CD40 expression in bone marrow-derived dendritic cells. These results suggest that mycelial extract-adjuvanted vaccines can confer cross-protection against variant H5N1 influenza viruses. The use of extracts of mycelia derived from edible mushrooms is proposed as a new safe and effective mucosal adjuvant for use for nasal vaccination against influenza virus infection. ***J. Med. Virol. 82:128–137, 2010.*** © 2009 Wiley-Liss, Inc.

KEY WORDS: avian influenza; adjuvant; immunoglobulin A; hetero-subtypic immunity

INTRODUCTION

When developing a vaccine, both prophylactic effectiveness and safety must be considered. The mucosal immune system of the respiratory tract, which is a primary site of influenza infection, is usually the first immunological barrier against influenza virus infection. The influenza virus is able to cause annual epidemics of influenza by altering the antigenic properties of its surface hemagglutinin (HA), the antigenic glycoprotein that is responsible for binding of the virus to sialic acids

Takeshi Ichinohe is the Research Fellow of the Japan Society for the Promotion of Science.

Grant sponsor: Ministry of Health, Labour and Welfare and Research on Health Sciences with emphasis on Drug Innovation (partial support).

Takeshi Ichinohe's present address is Department of Immunobiology, Yale University School of Medicine, 300 Cedar Street, TAC S640, New Haven, CT 06520.

*Correspondence to: Hideki Hasegawa, Influenza Virus Research Center and Department of Pathology, Research on Blood and Biological Products National Institute of Infectious Diseases, 4-7-1 Gakuen, Musashimurayama-shi, Tokyo 208-0011, Japan. E-mail: hasegawa@nih.go.jp

Accepted 2 September 2009

DOI 10.1002/jmv.21670

Published online in Wiley InterScience (www.interscience.wiley.com)

on the surface of susceptible cells. Inactivated vaccines against the influenza virus are administered parenterally to induce the production of anti-HA IgG antibodies that are highly protective against homologous virus infection, but less effective against heterologous virus infection [Ichinohe et al., 2008]. In contrast, a number of studies have shown that the mucosal immunity acquired through natural infection, which is mainly due to the secreted form of IgA in the respiratory tract, is more effective and provides greater cross-protection against virus infections than systemic immunity induced by parenteral vaccination in humans and mice [Asahi et al., 2002]. In this regard, induction of secreted IgA in the respiratory tract has a stronger potential to confer protection against unpredictable epidemics of influenza.

In the effort to develop effective intranasal vaccines, cholera toxin and *Escherichia coli* heat-labile toxin have been used as adjuvants to enhance the mucosal immune response [Tamura et al., 2005]. Although these toxins effectively provoke mucosal immune responses, they elicit adverse clinical side effects, such as nasal discharge and the facial paralysis of Bell's palsy [Mutsch et al., 2004]. Therefore, other adjuvants that are both effective and safe for human use have been developed for clinical application with intranasal influenza vaccine [Coulter et al., 2003; Hasegawa et al., 2005; Ichinohe et al., 2005, 2006, 2007a,b; Asahi-Ozaki et al., 2006].

It has been reported that extracts derived from certain mushrooms can elicit an innate immune response, resulting in activation of NF-κB, and strongly stimulate cellular and humoral immunity [Kim et al., 2003; Kuo et al., 2006]. These mushroom extracts induce phenotypic and functional maturation of dendritic cells, tumoricidal activity in macrophages, and augmentation of natural killer cell activity [Sorimachi et al., 2001; Kodama et al., 2005; Kim et al., 2006]. It has also been shown that oral administration of mushroom extracts has an anti-inflammatory effect [Bernardshaw et al., 2006] and decreases IgE levels through modulation of the Th1/Th2 balance [Inagaki et al., 2005; Lim et al., 2005]. In an experimental peritonitis model, mice that were treated orally with edible mushroom (*Agaricus blazei*) extracts prior to bacterial challenge showed significantly lower levels of septicemia and improved survival rates [Bernardshaw et al., 2006]. Extracts from these mushrooms also have been used in immunotherapy to prevent tumor growth and metastasis [Ukawa et al., 2000; Sanzen et al., 2001]. These findings prompted an investigation into whether the administration of intranasal influenza vaccine in combination with mushroom extracts would induce a protective immune response against a lethal and heterologous virus challenge. To accomplish this, the effectiveness of 12 mycelial extracts as an immune-enhancing adjuvant was assessed by comparison with the effects of the adjuvant, poly(I:C). The results of the present study demonstrate for the first time that intranasal administration of inactivated influenza virus vaccine in combination with mycelial extracts as a mucosal adjuvant induces cross-protective immune responses against homologous and heterologous variant influenza viruses, including highly pathogenic influenza A H5N1 virus isolates.

MATERIALS AND METHODS

Mice

Six- to 8-week-old female BALB/c mice were purchased from Japan SLC (Hamamatsu, Shizuoka, Japan). MyD88-deficient mice were kindly provided by Dr. Shizuo Akira (Osaka University, Osaka, Japan) [Adachi et al., 1998]. Mice were kept under specific pathogen-free conditions approved by the Institutional Animal Care and Use Committee of the National Institute of Infectious Diseases.

Vaccines and Influenza Viruses

HA vaccine (split-product virus vaccine) was prepared at the Kitasato Institute (Saitama, Japan) from members of the family Orthomyxoviridae, genus *Influenzavirus A, B*, species *Influenzavirus A*, including influenza A/PuertoRico/8/34 (A/PR8; H1N1). The virus was grown in allantoic cavities of 10- to 11-day-old fertile chicken eggs, purified and disintegrated with ethyl ether. The vaccines contained all proteins from the virus particle; however, the major component of the vaccine was HA (about 30% of the total protein). The A/PR8 virus used for the challenge experiments was adapted for use in mice by subculturing 148 times in ferret, 596 times in mouse, and 73 times in 10-day-old fertile chicken eggs.

The strains of influenza A virus H5N1 used in this study were A/Vietnam/1194/2004 and A/Indonesia/6/2005 [Gao et al., 1999]. The influenza A/Vietnam/1194/2004 virus and influenza A/Indonesia/6/2005 virus obtained from patients with H5N1 disease were propagated in 10-day-old embryonated chicken eggs for 2 days at 37°C. These viruses were stored at −80°C and viral titers were quantified by plaque assay using MDCK cells. The H5N1 vaccine used in these studies was NIBRG14, a formalin-inactivated whole virus vaccine derived from a recombinant avirulent avian virus containing modified HA and neuraminidase from the highly pathogenic avian influenza A/Vietnam/1194/2004 virus and other viral proteins from influenza A/PR/8/34 (H1N1) [Nicolson et al., 2005]. Modified HA lacks the multibasic amino acids at the cleavage site.

Preparation of Adjuvants

The mycelia extracts of *Phellinus linteus*, *Cordyceps militaris*, *Lyophyllum decastes*, *Macrolepiota gracilenta*, *Naematoloma sublateritium*, *A. blazei*, *Grifola frondosa*, *Ganoderma lucidum*, *Hericium erinaceum*, *Inonotus obliquus*, *Lentinula edodes*, and *Pleurotus nebrodensis* were kindly provided by Intelligence Biological Institute Co., Ltd (Nirasaki, Yamanashi, Japan). The extracts of mycelia were prepared as described previously [Inagaki et al., 2005]. Synthetic double-stranded RNA poly(I:C) was kindly provided by Toray

Industries, Inc. (Kamakura, Kanagawa, Japan). Lipopolysaccharide and Zymosan A from *Saccharomyces cerevisiae* were purchased from Sigma (St. Louis, MO).

Immunization and Infection

Five mice from each experimental group were anesthetized with diethyl ether and primarily immunized by dropping 1 μg of vaccine per mouse with various adjuvants into both nostril. Four weeks later, they were re-immunized in the same manner with the same adjuvant. For A/PR8 virus infection, two different infection protocols were used. Under the first protocol, each mouse was anesthetized and infected by intranasal application of 20 μl of virus suspension (1,000 PFU in PBS; 40 LD_{50}). This procedure induced total respiratory tract infection, which resulted in virus shedding from the nose and lungs, and led to death from viral pneumonia about 7 days later. Under the second protocol, anesthetized mice were infected by dropping 2 μl of virus suspension (1,000 PFU in PBS) into each nostril. The nasal-restricted volume (4 μl) of virus suspension induced nasally localized infection, which was not lethal. The nasal and lung wash virus titers were used as indices of protection in the upper and lower respiratory tracts of immunized mice, respectively. For infection with influenza A H5N1 virus, each mouse was anesthetized and 4 μl of PBS containing virus suspension with 1,000 PFU of H5N1 was administered intranasally (2 μl/nostril). The virus suspension remained in the local nasal area and could not enter the lung tissue, and the initial viral infection was limited to the nasal area, leading to death about 8 days later. H5N1 infection experiments were carried out in Biosafety Level 3 containment facilities, approved by the Guides for Animal Experiments Performed at National Institute of Infectious Diseases.

Measurement of Virus Titer and Antibody Titer

Serum, nasal washings, and bronchoalveolar washings were collected for measurement of virus titer and antibody titer from mice euthanized under anesthesia with chloroform. To collect nasal washings, a hypodermic needle was inserted into the posterior opening of the nasopharynx and 1 ml of PBS containing 0.1% bovine serum albumin was injected three times (1 ml total). Bronchoalveolar washings were collected by washing the trachea and lungs twice by injection of 1 ml PBS containing 0.1% BSA (2 ml total). The levels of IgA and IgG antibodies versus HA molecules purified from the A/PR8 viruses or NIBRG14 vaccine were determined by ELISA as described previously [Ichinohe et al., 2005, 2007a]. Briefly, ELISA was performed sequentially from the solid phase (EIA plates; Costar, Cambridge, MA) with a ladder of reagents as follows: first, HA molecules purified from influenza A/PR8 virus or NIBRG14; second, nasal washings, bronchoalveolar washings, or serum; third, either goat anti-mouse IgA antibody (α-chain specific; Amersham Biosciences, Piscataway, NJ) or goat anti-mouse IgG antibody (γ-chain-specific; Amersham Biosciences) conjugated with biotin; fourth, streptavidin conjugated with alkaline phosphatase (Life Technologies, Rockville, MD); and fifth, *p*-nitrophenylphosphate. The amount of chromogen produced was determined by measuring the absorbance at 405 nm using an ELISA reader. A twofold serial dilution of either purified A/PR8 HA-specific IgA (320 ng/ml) or A/PR8 HA-specific monoclonal IgG (160 ng/ml) was used as a standard, as described previously [Asahi et al., 2002]. The binding kinetics of the standard A/PR8 HA-specific monoclonal IgG was comparable with A/PR8 HA-specific IgG obtained from immunized mice. The A/PR8 HA-specific antibody concentration of each sample was determined from standard regression curves constructed for each assay with a programmed SJeia Autoreader (Model ER-8000; Sanko Junyaku, Tokyo, Japan). Standards for NIBRG14-reactive IgA and IgG antibody titration were prepared from the nasal washings or serum of survived mice after H5N1 virus challenge, and expressed using the same arbitrary units (160-unit). The NIBRG14-reactive antibody titer of each sample was determined from the standard regression curve constructed by twofold serial dilution of the 160-unit standard for each assay.

Before the hemagglutination inhibition tests, receptor-destroying enzyme (RDE II; Denka Seiken Co., Ltd, Tokyo, Japan) was added to the RBC-treated sera at 37°C overnight to inactivate non-specific hemagglutination inhibitors, followed by incubation at 56°C for 1 hr to inactivate RDE. Briefly, hemagglutination inhibition tests were performed by mixing 25 μl aliquots of serial twofold dilutions of the treated serum samples with four HA units of virus in microtiter plates and incubating them at room temperature for 30 min. Then, 50 μl of 0.5% chicken RBCs were added to each well and incubated at room temperature for 30–40 min. The hemagglutination inhibition titer was expressed as the reciprocal of the highest serum dilution that completely inhibited hemagglutination of four HA units of the virus.

The virus titer was measured as follows: 200 μl aliquots of serial 10-fold dilutions of the nasal washings were inoculated into MDCK cells in six-well plates. After incubation for 1 hr, each well was overlaid with 2 ml of agar medium. The number of plaques in each well was counted 2 days after inoculation. All experiments were repeated independently at least three times, and the data are presented as means ± SD.

Antigen-Specific T-Cell Response

Antigen-specific T-cell responses were measured as described previously [Ichinohe et al., 2005]. Spleens were harvested from mice 1 week after booster vaccination. After preparation of a single-cell suspension, T-cells were purified by depletion of $CD11b^+$ (Mac-1), $CD45R^+$ (B220), $DX5^+$, and $Ter\text{-}119^+$ cells using a magnetic cell sorter (MACS: Militenyi Biotec, Bergisch, Germany). To prepare antigen-presenting cells, splenocytes from normal BALB/c mice were depleted of